The Direct Initiation of Detonation in Decane-Air and Decane-Oxygen Sprays

M.J. Tang, J.A. Nicholls, M. Sichel and Z.C. Lin

Gas Dynamics Laboratories

Report No. UM-018404-1

October 1983

sponsored by

Army Research Office
Durham, N.C.

Contract No. DAAG 29-80-K-0040

Foreword

This report represents a portion of the research conducted under ARO Contract No. DAAG-29-80-K-0040, UM project number 018404. The program was supported by the Army Research Office, Durham, N.C. and conducted in the Gas Dynamics Laboratories, Department of Aerospace Engineering, The University of Michigan, Ann Arbor, Michigan. The effort extended over the period July 1, 1980 until July 1, 1983. Professors J. A. Nicholls and M. Sichel served as Co-Principal Investigators and Dr. Norman Slagg of ARRADCOM, Dover, N. J. as the Army technical monitor.

Abstract

The direct initiation of detonations in a decane spray with 400μm diameter droplets in air and oxygen has been studied using a vertical shock tube. The critical energy for the direct initiation of detonation has been measured for decane-air mixtures of equivalence ratios ϕ = 0.92, 1.18, 1.70, 2.49 and 3.27 and for decane-oxygen mixtures of ϕ = 0.24, 0.38 and 0.74. The lean detonability limit for a decane spray in air was determined to be ϕ = 0.92, i.e., 6% fuel (by mass), and that for a decane spray in oxygen was found to be not much leaner than ϕ = 0.24, i.e., 6.5% fuel (by mass).

Detonation is easily obtained in decane-oxygen mixtures and has been realized in decane-air mixtures over the equivalence ratio range of 0.92-3.27. There is a well defined minimum of the critical initiation energy for a decane-air mixture at a slightly rich composition ($\phi \simeq 1.2$). This value coincides with the maximum of the theoretically predicted heat release from the chemical reaction when dissociation is taken into account.

Table of Contents

List of Tables

List of Figures

I. Introduction

Two of the most important parameters of two-phase detonations are the critical initiation energy and the detonability limits. Only a few researchers have measured these two parameters in sprays. Bull et al. [1] obtained critical initiation energy and detonability data for hexane sprays in a 5 m^3 bag, using a high explosive charge as the initiator. They reported that dodecane and decane could not be detonated, even by relatively large initiator charges. Dabora [2] reported the determination of the lean limit of kerosene-air mixtures sensitized by the addition of propyl nitrate (PN) and butyl nitrate (BN) using a vertical shock tube. Bar-Or [3] observed the initiation of detonation of a decane spray in oxygen and oxygen enriched air in a sectored tube. However, no systematic studies have been made of the critical initiation energy and detonability limits of decane sprays in air or oxygen.

The purpose of this report is, thus, to present the results of a systematic experimental study of the critical initiation energy for the direct initiation of decane-air and decane-oxygen mixtures in a vertical shock tube. An upper and lower value of the critical initiation energy of decane-air and decane-oxygen mixtures has been determined at a number of equivalence ratios. The upper value of the critical initiation energy, E_{cu}, is defined as the minimum initiation energy above which the direct initiation of detonation is observed 100% of the time and the lower value of the critical initiation energy, $E_{c\ell}$, is defined as the value below which detonation never occurs. For initiation energies between these two values the percentage of the occurrence of detonation is variable and different types of velocity trajectories corresponding to different initiation mechanisms have been observed.

The lean detonability limit, defined as the composition that requires almost an order of magnitude higher initiation energy than the minimum value, has been determined experimentally. Unfortunately, the rich detonability limit, requiring almost an order of magnitude higher initiation energy than the minimum could not be determined by the experiments. The equivalence ratio could not be increased beyond $\phi = 3.27$ for decane in air and $\phi = 0.74$ for

decane in oxygen because of the space limitation of the arrangement of the drop generation system

A key problem is to relate the experimentally measured initial pressure in the H_2-O_2-He initiator to the energy which is actually transmitted to the spray. An estimate of the transmitted energy is developed.

II. Experimental Apparatus

The experiments were conducted in a vertical shock tube of length 8.2 m and with a square cross-section of 4.13 cm x 4.13 cm as shown in Fig. 1.

Monodisperse drops are produced at the top of the tube by a drop generator. Hypodermic needles with 210 μm inner diameter were used throughout this study to generate monodisperse 400 μm diameter droplets. The theory and operation of the drop generator were discussed by Dabora [4] and Pierce [5]. Approximately 85% of the terminal velocity of the drops was chosen as the exit velocity of the liquid jet. The hypodermic needles were vibrated at the Rayleigh frequency (2150 Hz) throughout the experiments.

An average loss of 25% of the fuel on the walls of the tube was observed in the experiments which undoubtedly reduced the actual fuel-oxidizer ratio along the tube. To compensate for this effect, the loss-less fuel-oxidizer ratio was reduced. Since the fuel sticking on the walls may still play a role in the chemical reaction due to film detonation, a reduction of 15% of the fuel-oxidizer ratio was used instead of 25%; however, this choice is somewhat arbitrary.

The blast wave initiator consisted of a 5 cm diameter shock tube 1.2 m long mounted just below the drop generator at an angle of 15° to the main tube. For all tests the initiator was filled with a mixture of hydrogen, oxygen and helium (2:1:1 by volume) with pressures ranging from 1 atm to 8 atm, and a detonation was initiated in the tube using a glow plug at the closed end.

The wave position was sensed by 11 pressure switches placed along the main tube at 0.5 m intervals. The output from the switches was fed to a raster circuit, with the raster trace being triggered by the first pressure

switch located immediately behind the diaphragm at the end of the initiator. The pressure switches are described in [3] and were carefully adjusted before each run to ensure electrical contact at shock arrival.

The pressure profiles behind shock and detonation waves were measured in each run using two Kistler piezo-electric pressure transducers with built-in amplifiers placed 3 m and 4.5 m from the first pressure switch. Signals were recorded using a Tektronix type 555 dual beam time base oscilloscope, and were triggered 0.5 m before each transducer.

Experimental runs were conducted as follows: the tube was purged with compressed air for 20 minutes to ensure a dry wall before each run and then fresh air was introduced into the tube. For oxygen or oxygen-enriched air, the tube was filled with the desired gas after purging the tube with air. The initiator was filled with the premixed H_2-O_2-He mixture to the desired pressure. A mechanical timer was used to start the drop generator eight seconds before the firing of the initiator glow-plug. The ball valve used to protect the drop generator from the shock wave was operated automatically via a solenoid valve connected to the same mechanical timer to insure the time sequence.

III. Theoretical Prediction

1. The Calculation of Theoretical C-J Parameters

Theoretical values of the detonation parameters in an all-gaseous mixture for decane in air and in oxygen were calculated using the Bordon McBride computer code [6]. In calculating the detonation parameters, an equivalent premixed, all-gaseous combustible mixture is assumed, but the enthalpy of formation used is that for the liquid. Some results of the calculation for decane in air and in oxygen are listed in Tables 1 and 2, respectively.

In Tables 1 and 2, the subscripts 0 and 2 refer to properties in the unburned mixture and at the C-J plane, respectively. M_{CJ} was calculated from $M_{CJ} = D_{CJ}/a_1$, where a_1 is the speed of sound in the oxidizer, with a_1 = 346 m/s in air, 331 m/s in oxygen. The calculated C-J velocities and C-J pressures for both decane in air and in oxygen as functions of equivalence

ratios are plotted in Figs. 2 and 3. It is obvious that the maximum values of the C-J velocity and the C-J pressure for decane-air mixtures do not occur at the stoichiometric composition with $\phi = 1$ but rather for a rich mixture with $\phi = 1.25 \sim 1.30$. For decane-oxygen mixtures the maximum velocity occurs for the compositions with $\phi = 2.0 \sim 2.1$. It can be seen from the curves of C-J velocity, D_{CJ}, and C-J pressure, P_{CJ}, versus equivalence ratio that D_{CJ} and P_{CJ} decrease more rapidly with the decreasing of ϕ on the lean side than that with the increasing ϕ on the rich side of the maximum. The reason for this is that for the leaner mixtures the lower values of D_{CJ} are due to reduced heat release because of less fuel, an effect that varies strongly with ϕ. For the richer mixtures D_{CJ} becomes smaller because there is insufficient O_2 for complete combustion, an effect that is less sensitive to ϕ.

The variation of the calculated C-J velocity with fuel/oxidizer ratio (by mass) is presented in Fig. 4. Figure 4 shows that the range of compositions which correspond to sufficient heat release to allow detonation is quite wide for decane-O_2 mixtures, while the composition range for decane-air is relatively narrow. This suggests that the range of detonable compositions for decane-O_2 mixtures will be much wider than for decane-air mixtures.

Since the reaction zone length in two-phase detonations can be quite large, a significant velocity deficit due to wall losses is to be expected. The velocity deficit due to losses of heat and drag can be approximated using the analytical expression derived by Ragland et al. [7] for a one-dimensional two-phase detonation in a shock tube.

The assumptions used are as follows: a) The frictional drag and heat loss through the wall were considered to be distributed uniformly over the cross-section of the tube, thereby reducing the detonation velocity. Therefore, the flow can be treated as one-dimensional. b) All of the liquid is consumed and enters the control volume before the end of the reaction zone. c) For a dilute spray the equations of state and speed of sound are defined in terms of the gas phase and the gases are both thermally and calorically perfect.

By extending the Rankine-Hugoniot relations to account for heat and momentum transfer out of the reaction zone as well as mass and heat addition within the reaction zone, Ragland et al. obtained the result:

$$\frac{u_s}{(u_s)_o} = \left\{1 + [C_D + 2(\gamma_2^2 - 1)C_H]\ (\frac{1}{1+\psi})(\frac{A_s}{A_c}) \cdot \frac{u_1^2}{u_s(u_s - u_1)}\right\}^{-1/2} \quad (1)$$

where u_s is the detonation velocity with losses taken into account, $(u_s)_o$ is the ideal C-J velocity without losses, γ_2 is the ratio of specific heats at the C-J plane, A_s is the area through which the heat and momentum transfer occur, A_c is the cross-sectional area of the tube, ψ is the fuel-to-oxidizer mass ratio, u_1 is the flow velocity immediately behind the shock wave, and C_D and C_H are the drag and heat transfer coefficients, respectively.

If it is assumed that Reynold's analogy holds, so that $C_D = 2C_H$, and the normal shock relations for a perfect gas are used to replace u_1 by u_s, Eq. (1) becomes

$$\frac{u_s}{(u_s)_o} = \left\{1 + \frac{128\ \gamma_2^2\ C_H\ t_3}{(1+\psi)(\gamma_o + 1)b}\ \frac{(u_s^2 - a_o^2)^2}{u_s[(\gamma_1 - 1)u_s^2 + 2a_o^2]}\right\}^{-1/2} \quad (2)$$

where b is the perimeter of the tube. Then $A_c = (1/16)\ b^2$ and $A_s = b\ u_s\ t_3 = b\ \ell_R$, where t_3 is the time after passage of the shock front until completion of the deformation, vaporization, diffusion and chemical reaction of the fuel, and ℓ_R is the reaction zone length.

From the experimental results of Bar-Or [3], it follows that $t_3 \tilde{=} 50\mu s$ and $C_H \tilde{=} 2.5 \times 10^{-3}$ for the decane-O_2 mixture and $t_3 = 100\ \mu s$, $C_H = 2.5 \times 10^{-3}$ for the decane-air mixture.

The detonation velocities calculated by using Eq. (2) and the Gordon McBride code for $(u_s)_o$ are listed in Tables 3 and 4 for decane-air and decane-O_2 mixtures, respectively. These values are plotted in Fig. 5.

The effect of the choices of C_H and t_3 on the detonation velocity is shown in Figs. 6 and 7 respectively for decane-O_2 mixtures. In general the D_{CJ} decreases about one percent when C_H increases 0.5×10^{-3} or when t_3 increases 10 μs. In the range of possible values of C_H and t_3, the reduction of D_{CJ} from the gaseous mixture varies from six percent to 15%. Nevertheless,

the shape of the curve of D_{CJ} versus ϕ is similar to that computed using the Gordon McBride code for the all-gaseous case as shown in Fig. 5.

Gubin and Sichel [8] suggested that the deficit of the detonation velocit is not due to the heat and drag losses from the reaction zone but is mainly due to incomplete fuel reaction between the shock and the C-J plane.

Gubin and Sichel [8] assumed that the fuel which is stripped from the droplets is rapidly vaporized and all burns after the chemical induction time of the fuel vapor, and that only this fuel contributes to the heat release between the shock and C-J plane. The unstripped portion of the fuel, which remains as part of the drop, burns downstream of the C-J plane and is assumed to make no contribution to the propagation velocity. Using empirical results for the stripping rates and the induction time of the gaseous fuel, Gubin and Sichel [8] were then able to compute the propagation velocity. The velocity will depend on the equivalence ratio and the droplet diameter; calculations were made for kerosene droplets in oxygen.

The stripping mechanism, as well as the chemical induction time, of liquid hydrocarbon fuels is not overly sensitive to the fuel type. The resul of Gubin and Sichel were therefore used to determine the reduction of the C-J velocity of the decane spray below the all-gaseous value obtained from the Gordon McBride [6] code.

The calculated value of D_{CJ} using the different methods described above are listed in Tables 5 and 6 and are plotted in Figs. 8 and 9 with the experimental data for comparison. The tables and figures show that the calculated values of D_{CJ}, taking into account the heat and drag losses as well as incomplete combustion, are in agreement with the experimental results of lean decane-O_2 mixtures. However, none of the theoretical calculations of D_{CJ} are in agreement with the experimental results of rich decane-air mixtures, although the general behavior of the data again suggests incomplete combustior as a partial explanation of the velocity deficit. It probably is inappropriat in any case to apply the Gubin-Sichel results, computed for O_2, to air. Replacing O_2 with air in the Gubin-Sichel [8] analysis will increase the induc tion time as well as the heat release in the reaction zone and this effect would shift the theoretical curve toward better agreement with the measured values of D_{CJ}. More detailed analysis is obviously required in this case.

2. The Estimation of Initiation Energy Level

In the initiation of spray detonation, the indicator used for comparing initiation energies was the initial pressure in the initiator. In order to relate the initial pressure in the H_2-O_2-He initiator to the energy transmitted to the spray, the total chemical energy released in the initiator was calculated by means of the chemical reaction equation provided by the Gordon McBride code [6], which takes dissociation into account. The calculated initiation energies and energy densities for various initiator pressure are tabulated in Table 7 and the details of the calculation are described in a previous report [9]. Here initiation energy density refers to the initiation energy transmitted per unit area of the main tube. Since the same initiator was used throughout the experiments, the initiation energy density can characterize the initiation phenomena. Of course, the energy calculated this way is not necessarily equal to the energy actually transmitted to the spray detonation tube, but gives an indication of relative magnitude for different initiator pressures.

3. The Calculation of Shock Wave Decay

In order to determine the establishment of detonation, the trajectories of the shock front propagating into nonreactive mixtures were first calculated and measured [9]. In the calculation the initiator is considered as the driver and the main tube as the driven section of a shock tube. It is assumed that the burned mixture in the initiation tube has reached a uniform state before the break-up of the diaphragm. Since the time interval between ignition of the gaseous mixture and the break-up of the diaphragm is much longer than the time for detonation transit through the initiator tube, the constant entropy equation was used to determine the pressure in the driver section. The equations of shock tube performance for an ideal gas [10], including the effect of the area change near the diaphragm [11], [12], were then used to determine the initial Mach number in the driven section and the distance, at which the rarefaction catches up with the shock front. The calculated initial Mach number, M_1, corresponding to various pressure ratios, p_4/p_1, is compared to the measured value in Fig. 10.

It is assumed that after the rarefaction wave catches up with the shock front the wave can be treated as a constant energy blast wave so that its decay in nonreactive mixtures can be calculated approximately by using the equation for a planar blast wave given by Dabora [2]. The trajectories of the shock front obtained both from this calculation and from the experiments in nonreactive mixtures are plotted in Fig. 11. Good agreement is shown between the experimental data and the calculated values, especially for intermediate initiation energy levels.

IV. Experimental Results

1. The Critical Initiation Energy

In order to determine the initiation behavior of decane sprays in air, experiments were performed on mixtures with equivalence ratios ϕ = 0.92, 1.18, 1.70, 2.49 and 3.27, which correspond to drop generator operation with 7, 9, 13, 19 and 25 hypodermic needles. For different compositions the energy inputs were varied over the range 3.96×10^6 j/m^2 to 33.1×10^6 J/m^2, corresponding to initiator pressures ranging from 1 atm to 8 atm absolute (the firing of the initiator was irregular below 1 atm and operation with pressures above 8 atm was considered unsafe).

For comparison, experiments of the direct initiation of a decane spray in pure oxygen were performed for 5 compositions, corresponding to ϕ = 0.24, 0.27, 0.38, 0.56 and 0.74. The low values of the equivalence ratio is due to the fact that for a given fuel injection rate the total volume of gas in the tube is the same as in the air case but now consists entirely of oxygen.

In the experiments, two values of the critical initiation energy were determined for each mixture. The upper value, E_{cu}, is defined as the lowest initiation energy (or lowest initiator pressure) leading to direct initiation 100% of the time (for at least 6 runs). The lower value, $E_{c\ell}$, is defined as the highest energy level (or highest initiator pressure) at which detonation was never generated (in at least 6 runs).

The upper and lower values of the critical initiation energy obtained in the experiments for decane spray in air and in oxygen corresponding to various equivalence ratios are tabulated in Tables 8 and 9 and plotted in Figs. 12 and 13. For decane sprays in pure oxygen lower values of the critical initiation energy could not be found in the experiments, because detonation always occurred, even at very low initiator pressures.

It can be seen from Fig. 12 that for decane spray in air there is a well defined minimum of E_{cu}, 9.23 x 10^6 Joule/m^2, at a slightly rich composition ($\phi \simeq 1.2$) corresponding to that for the maximum detonation velocity and pressure as shown in Figs. 2 and 3. On the lean side, E_{cu} rises very rapidly with the decrease of ϕ; however, on the rich side, the increase in E_{cu} is more gradual. This behavior which is similar to that observed in the case of gaseous detonations [3], is related to the variation of the induction zone length for lean and rich mixtures.

2. The Detonability Limits

The lean detonability limit is defined as the composition that requires nearly an order of magnitude higher initiation energy than what is required to initiate the richer mixtures. For decane-air mixtures this limit has been found experimentally to correspond to an equivalence ratio of $\phi = 0.92$. At this composition, E_{cu} is 33.1 x 10^6 Joule/m^2 (or 7.81 atm initiator pressure). This is the highest initiation energy level available in this experimental apparatus, and is at least three times the minimum value of 10.6 x 10^6 Joule/m^2. The rich detonability limit, which is defined as the composition that requires nearly an order of magnitude higher initiation energy than the minimum value, could not be determined, because the apparatus was limited to 25 fuel streams, corresponding to an equivalence ratio of 3.27. For this mixture, the direct initiation of detonation was achieved at E_{cu} = 16.47 x 10^6 Joule/m^2 (4.06 atm initiator pressure), which is not much higher than the minimum required value.

The lean limit observed here is richer than the value of $\phi = 0.8$ observed by Bull [1] for hexane and the value of $\phi = 0.65$ observed by Lu et al. [14] for heptane fog. The very low vapor pressure of decane may account for this difference.

For decane sprays in oxygen, it appears that the lean limit is not much leaner than a composition corresponding to $\phi = 0.24$. The five decane-oxygen mixtures tested were all on the lean side. According to the theoretical prediction, the range of detonable compositions of decane-oxygen mixtures should be much wider than that of decane-air mixtures. Therefore, the rich limit must be far beyond the compositions which would be produced in this experimental appratus.

For comparison, the upper value of the critical energy, E_{cu}, versus fuel-oxidizer mass ratio for both decane-air and decane-oxygen mixtures were plotted in Fig. 14. It appears that the lean composition limits of decane-air and decane-O_2 mixtures are approximately the same if presented in fuel-oxidizer ratio or the percentage of fuel.

3. The Propagation Velocity and Pressure Profile

Seven types of velocity trajectories were observed corresponding to different initiation energy levels, as shown in Fig. 15. Nevertheless, only typ 1 and type 2 were considered to represent direct initiation. For initiation energy at or above E_{cu}, the velocity trajectories were, therefore, all of typ 1 or type 2. The propagation velocity versus distance at E_{cu} for decane-air and decane-O_2 mixtures of various equivalence ratios are tabulated in Tables 10 and 11 and plotted in Figs. 16 and 17, respectively. The corresponding pressure traces are shown in Figs. 18 and 19.

In Tables 10 and 11, the average values of the propagation velocities of the runs under the same conditions as well as the standard deviations are pre sented. Since the standard deviations are very small they could not be presented in the figures.

For comparison, the experimental propagation velocities and the theoreti cal C-J values for gaseous mixtures of decane-air and decane-O_2 are presented in Tables 12 and 13. In these tables the propagation velocities measured at the end of the tube were taken as the experimental values. In addition, the velocities of the decaying shock fronts in nonreactive mixtures measured at the end of the tube, are also presented in these same tables.

The critical blast wave radius, R*, within which the energy released by combustion equals the critical blast wave energy, E_{cu}, is also presented in Tables 12 and 13, as calculated by the equation [15]

$$R^* = \frac{E_{cu}}{2Q\rho_o}$$

for the planar case, where E_{cu} is the critical blast wave energy per unit area of the main tube; ρ_o is the density of the unburned mixture and Q is the heat of combustion of the mixture per unit mass. Q is calculated from the Zeldovitch relation:

$$Q = \frac{D_{CJ}^2}{2(\gamma^2-1)}$$

Here the detonation velocity D_{CJ} is the measured value while the ratio of specific heats γ is taken from the calculation using the Gordon-McBride code and assuming gaseous fuel.

Regions of "steady" propagation velocity were attained towards the end of the tube for 4 decane-air mixtures (ϕ = 1.18, 1.70, 2.49 and 3.27) and for 5 decane-O_2 mixtures (ϕ = 0.24, 0.27, 0.28, 0.56 and 0.74). However, a slight velocity decay is still evident (about one percent) at the end of the tube. This indicates that the effect of the initiation source still comes into play.

Surprisingly, the propagation velocities corresponding to different compositions of rich decane-air mixtures at E_{cu} approached almost the same value towards the end of the tube, so that the velocity deficit, which is the difference between the theoretical C-J velocity of all gaseous mixtures and the experimental propagation velocity, decreased with increasing ϕ on the rich side. Furthermore, for the very rich mixture, ϕ = 3.27, the experimental propagation velocity is even higher than the theoretical value of the all-gaseous mixture, as shown in Table 12. The decrease of velocity deficit is probably mainly attributable to the fact that E_{cu} is higher for richer mixtures and the incomplete combustion of the very rich mixture which may reduce the amount of effective fuel.

Tables 14 and 15 show the experimental propagation velocities of 5 decane-air mixtures and 4 decane-O_2 mixtures at a constant initiation energy level (above E_{cu}). Comparison of the magnitudes of these velocities with those

listed in Tables 10 and 11 indicates that there is some influence from the initiation source, although it does not seem to be significant.

For decane-air mixtures, it can be seen from Table 14 and Fig. 20 that propagation velocities at the same initiation energy level above E_{cu} (4.40 atm initiator pressure) decreased slightly with increasing ϕ for mixtures of $\phi > 1.18$ during the first stage of propagation. However, the velocities having the same value at the tube inlet approached almost the same value towards the end of the tube.

It is clear that for the decane-O_2 mixtures at the same initiation energy level above E_{cu}, propagation velocities increased with increasing ϕ, on the lean side, as shown in Table 15 and Fig. 21.

V. Discussion and Conclusions

Detonations have been initiated in decane sprays in both air and oxygen using a detonation tube as the initiator. The critical initiation energy was determined over a wide range of compositions and the lean detonation limits were determined in air and oxygen. For the decane-air mixtures the lean limit was near the stoichiometric mixture ratio, that is, for $\phi = 0.92$, so that detonations were only observed in rich mixtures. For the decane-O_2 mixtures, the lean limit was found to be at the low equivalence ratio value of 0.24.

The theoretical prediction of the detonation velocity using a model which takes into account the heat and viscous losses in the reaction zone as well as the incomplete combustion of the spray droplets is in excellent agreement with the experimental results for lean decane-O_2 mixtures. Surprisingly, the experimental propagation velocities for rich decane-air mixtures are almost independent of the equivalence ratio and approach a constant value, which is even higher than the theoretical C-J value of a very rich all-gaseous mixture. It is suggested that the incomplete combustion may play an important role in the rich decane-air case and a detailed analysis is obviously required.

The investigation clearly shows that there are significant differences in the propagations and initiation of spray and all-gaseous detonations.

References

1. Bull, D. C. et al. "Detonation of unconfined fuel aerosols." Gasdynamics of Detonations and Explosions, vol. 75, Progress in Astronautics and and Aeronautics, pp. 48-60, 1981.

2. Dabora, E. K. Effect of Additives on the Lean Detonation Limit of Kerosene in Air. Final Report to U.S. Army Research Office, Grant No. DAAG-29-78-G0074.

3. Bar-Or, R. Cylindrical, Two Phase Detonations in Monodisperse Sprays. Doctoral Thesis, The University of Michigan, 1979.

4. Dabora, E. K. "Production of monodisperse sprays." The Review of Scientific Instruments, vol. 38, no. 4, pp. 502-506, April 1967.

5. Pierce, T. H. "Production of polydisperse sprays." The Review of Scientific Instruments, vol. 42, no. 11, pp. 1648-1649, November 1971.

6. Gordon, S. and McBride, B. Computer Program for Calculation of Complex Chemical Equilibrium Compositions, Rocket Performance, Incident and Reflected Shocks, and Chapman-Jouguet Detonations. NASA SP-273, 1971.

7. Ragland, K. W., Dabora, E. K. and Nicholls, J. A. "Observed structure of spray detonations." The Physics of Fluids, vol. 11, no. 11, November 1968.

8. Gubin, S. A. and Sichel, M. "Calculations of the detonation velocity of a mixture of liquid fuel droplets and a gaseous oxidizer." Combustion Science and Technology, vol. 17, pp. 109-111, 1977.

9. Tang, M. J. The Estimation of Initiation Energy Level and Shock Wave Decay. Technical Report, The University of Michigan, UM 018404-2, 1983.

10. Gaydon, A. G. and Hurle, I. R. The Shock Tube in High-Temperature Chemical Physics, Chapman and Hall, Ltd., London, 1963, pp. 20.

11. Bradley, J. N. Shock Waves in Chemistry and Physics, Methuen and Co., Ltd., London, 1962, p. 124.

12. Glass, I. I. and Gordon-Hall, J. Handbook of Supersonic Aerodynamics, Section 18, pp. 434.

13. Lee, J. H. "Initiation of gaseous detonation." Ann. Rev. Phys. Chem., 1977, 28:75-104.

14. Lu, P. L. et al. "Relations of chemical and physical processes in two-phase detonation." Acta Astronautica, vol. 6 pp. 815-826 (1979).

15. Nicholls, J. A. et al. "Theoretical and experimental study of cylindrical shock and heterogeneous detonation waves." Acta Astronautica, vol. 1, pp. 385-404 (1974).

Table 1. Detonation properties of decane in air (according to Gordon McBride)

Percent fuel	F/O	ϕ	P_2/P_o	T_2/T_o	ρ_0/ρ_2	H (cal/gm)	γ_s	γ_2	a_2 (m/s)	D_{cJ} (m/s)	M_{cJ}
2.05	0.0210	0.314	8.883	5.159	1.690	118.1	1.287	1.287	756	1278	3.69
2.94	0.0303	0.453	11.510	6.495	1.725	154.2	1.260	1.260	840	1449	4.19
4.24	0.0443	0.662	14.965	8.125	1.766	199.2	1.218	1.219	926	1635	4.72
4.73	0.0496	0.743	16.109	8.606	1.782	213.2	1.199	1.202	947	1687	4.88
5.51	0.0583	0.872	17.632	9.174	1.803	230.8	1.175	1.181	972	1752	5.06
5.78	0.0613	0.917	18.065	9.316	1.807	235.4	1.170	1.177	979	1770	5.11
6.27	0.0668	1.000	18.711	9.504	1.812	241.8	1.165	1.174	991	1796	5.19
6.55	0.0701	1.048	18.998	9.573	1.813	244.3	1.165	1.174	997	1808	5.23
6.69	0.0717	1.073	19.121	9.596	1.813	245.3	1.166	1.175	1000	1813	5.24
7.30	0.0787	1.178	19.451	9.613	1.806	246.6	1.176	1.183	1012	1829	5.29
8.51	0.0930	1.391	19.341	9.292	1.781	238.5	1.215	1.217	1028	1830	5.29
9.49	0.105	1.568	18.933	8.844	1.765	226.9	1.238	1.240	1027	1813	5.24
10.22	0.114	1.702	18.576	8.479	1.757	217.3	1.250	1.251	1022	1795	5.19
11.84	0.134	2.009	17.664	7.642	1.743	194.2	1.270	1.270	1001	1744	5.04
14.26	0.166	2.488	15.996	6.398	1.725	155.8	1.293	1.293	955	1648	4.76
16.41	0.196	2.937	14.162	5.304	1.708	117.4	1.312	1.313	901	1540	4.45
17.96	0.219	3.274	13.514	4.877	1.715	99.0	1.295	1.303	867	1487	4.30
20.53	0.258	3.865	13.234	4.569	1.729	79.7	1.268	1.283	835	1444	4.17

Table 2

Detonation properties of decane in oxygen (according to Gordon McBride)

Percent Fuel	F/O	ϕ	p_2/p_o	T_2/T_o	ρ_o/ρ_2	H (cal/gm)	γ_s	γ_2	a_2 (m/s)	D_{CJ} (m/s)	M_{CJ}
5.61	0.0594	0.207	18.525	9.505	1.810	217.4	1.168	1.175	941	1703	5.15
6.34	0.0677	0.236	19.832	9.948	1.822	230.2	1.156	1.168	963	1754	5.30
7.09	0.0763	0.266	21.031	10.316	1.830	241.3	1.148	1.164	983	1798	5.43
7.41	0.0800	0.279	21.508	10.452	1.832	245.6	1.146	1.164	991	1816	5.49
8.26	0.0900	0.314	22.729	10.776	1.838	256.1	1.141	1.165	1011	1859	5.62
9.92	0.110	0.384	24.953	11.277	1.846	274.0	1.135	1.170	1048	1934	5.84
11.50	0.130	0.453	26.953	11.647	1.850	288.9	1.133	1.178	1079	1996	6.03
13.86	0.161	0.561	29.871	12.081	1.854	309.1	1.132	1.191	1123	2082	6.29
15.97	0.190	0.662	32.470	12.385	1.856	325.8	1.132	1.201	1160	2152	6.50
17.47	0.212	0.738	34.342	12.568	1.857	337.3	1.133	1.208	1185	2200	6.65
17.56	0.213	0.743	34.455	12.578	1.857	338.0	1.133	1.208	1186	2203	6.65
20.00	0.250	0.872	37.540	12.820	1.858	355.8	1.134	1.217	1225	2276	6.88
22.29	0.287	1.000	40.495	12.994	1.859	371.7	1.136	1.222	1260	2341	7.07
23.50	0.307	1.071	42.065	13.063	1.859	379.7	1.137	1.224	1277	2373	7.17
28.53	0.399	1.391	48.574	13.156	1.857	408.2	1.143	1.218	1344	2494	7.54
31.03	0.450	1.568	51.555	13.038	1.854	417.1	1.149	1.209	1371	2542	7.68
36.56	0.576	2.009	56.031	12.165	1.836	410.6	1.174	1.199	1410	2590	7.82
37.18	0.592	2.063	56.251	12.005	1.833	406.7	1.179	1.200	1412	2589	7.82
41.77	0.717	2.500	55.518	10.441	1.804	355.3	1.221	1.227	1403	2531	7.65
45.73	0.843	2.937	50.791	8.564	1.770	273.9	1.273	1.274	1352	2392	7.23
46.26	0.861	3.000	49.852	8.283	1.766	260.5	1.280	1.281	1340	2366	7.15
50.10	1.004	3.500	49.437	7.059	1.768	183.8	1.273	1.280	1245	2201	6.65
52.58	1.109	3.865	43.201	6.492	1.768	141.9	1.273	1.283	1195	2112	6.38

Table 3

Detonation velocity of 400 μm decane-air mixture (with wall losses

Equivalence ratio ϕ	Fuel-oxidizer ratio F/O	D_{C-J} (m/sec) (all gases)	γ_2 (all gases)	D_{C-J} (m/s) (with wall losses)
0.314	0.0210	1278	1.287	1153
0.453	0.0303	1449	1.260	1299
0.662	0.0443	1635	1.219	1440
0.743	0.0496	1687	1.202	1487
0.872	0.0583	1752	1.181	1537
0.917	0.0613	1770	1.177	1555
1.000	0.0668	1796	1.174	1576
1.073	0.0717	1813	1.175	1588
1.178	0.0787	1829	1.183	1600
1.391	0.0930	1830	1.217	1590
1.568	0.1050	1830	1.240	1578
1.702	0.1140	1795	1.251	1560
2.009	0.1340	1744	1.270	1524
2.488	0.1660	1648	1.293	1450
2.937	0.1960	1540	1.313	1365
3.274	0.2190	1487	1.303	1330
3.865	0.2580	1444	1.283	1304

$C_H = 2.5 \times 10^{-3}$

$t_3 = 100$ μs

Table 4

Detonation velocity of 400 μm decane-O_2 mixture
(with wall losses)

Equivalence Ratio ϕ	Fuel-Oxidizer ratio F/O	D_{C-J} (m/sec) (all gases)	γ_2 (all gases)	D_{C-J} (m/sec) (with losses)
0.207	0.0594	1703	1.175	1583
0.236	0.0677	1754	1.168	1630
0.266	0.0763	1798	1.164	1670
0.279	0.0800	1816	1.164	1681
0.384	0.1100	1934	1.170	1785
0.453	0.1300	1996	1.178	1836
0.561	0.1610	2082	1.191	1910
0.662	0.1900	2152	1.201	1967
0.738	0.2120	2200	1.208	2010
0.743	0.2130	2203	1.208	2008
0.872	0.2500	2276	1.217	2071
1.000	0.2870	2341	1.222	2126
1.071	0.3070	2373	1.224	2155
1.391	0.3990	2494	1.218	2270
1.568	0.450	2542	1.209	2316
2.009	0.576	2590	1.199	2372
2.500	0.717	2531	1.227	2331
3.000	0.861	2366	1.281	2191
3.500	1.004	2201	1.280	2060
3.865	1.109	2112	1.283	1987

$C_H = 2.5 \times 10^{-3}$

$t_3 = 50\mu s$

Table 5

C-J velocity versus ϕ for decane-air mixture
(according to different methods)

ϕ · Equivalence ratio	0.92	1.18	1.70	2.49	3.27
According to Gordon-McBride	1770	1829	1795	1648	1487
According to Ragland & Nicholls ($C_H=2.5\times10^{-3}$, $t_3=100\mu s$)	1555	1600	1560	1450	1330
According to Gubin & Sichel	1328	1344	1436	1380	1245
Experimental Data	1388	1516	1543	1542	1555

Table 6

C-J velocity versus ϕ for decane-O_2 mixture
(according to different methods)

ϕ Equivalence Ratio	0.236	0.266	0.384	0.561	0.738
According to Gordon-McBride	1754	1798	1934	2082	2200
According to Ragland & Nicholls ($C_H=2.5\times10^{-3}$ $t_3=50$ μs)	1630	1670	1785	1910	2010
According to Gubin & Sichel	1565	1604	1735	1791	1848
According to Ragland & Gubin	1454	1490	1601	1643	1688
Experimental Data	1496	1500	1573	1697	1742

Table 7

Calculated energies released in H_2-O_2-He initiator

Initial pressure in initiator (atm)	Total mass of gaseous mixture in initiator (gm)	Energy released per unit mass (cal/gm)	Total energy released in initiator (cal)	Initiation energy density (MJ/m^2)
1.07	1.06	1530	1614	3.96
1.68	1.66	1581	2618	6.43
2.02	1.99	1597	3182	7.81
2.36	2.33	1615	3757	9.23
2.70	2.66	1629	4337	10.65
3.04	3.00	1643	4923	12.09
3.38	3.33	1654	5514	13.54
4.06	4.00	1675	6705	16.47
4.40	4.34	1687	7318	17.97
5.76	5.68	1715	9739	23.92
7.81	7.70	1750	13477	33.10

Table 8

Critical initiation energy
(decane/air - 400μm drops)

Number of Fuel Streams	7	9	13	19	25
Percentage of Fuel (by mass)	5.78	7.30	10.22	14.26	17.96
Fuel/oxidizer Ratio (by mass)	0.061	0.079	0.114	0.166	0.219
Equivalence Ratio	0.92	1.18	1.70	2.49	3.27
Upper critical energy, E_{cu}					
initiator pressure (atm)	7.81	2.36	2.70	3.38	4.06
initiator energy density (MJ/m^2)	33.10	9.23	10.65	13.54	16.47
Lower critical energy, $E_{c\ell}$					
initiator pressure (atm)	---	1.07	---	2.36	2.49
initiator energy density (MJ/m^2)	---	3.96	---	9.23	13.54

Table 9

Critical initiation energy
(decane/oxygen - 400 m drops)

Number of Fuel Streams	8	9	13	19	25
Percentage of Fuel (by mass)	6.34	7.09	9.92	13.86	17.47
Fuel/oxidizer Ratio (by mass)	0.068	0.076	0.110	0.161	0.212
Equivalence Ratio	0.24	0.27	0.38	0.56	0.74
Upper critical energy, E_{cu}					
initiatiator pressure (atm)	5.76	2.02	2.02	2.02	2.02
initiator energy density (MJ/m^2)	23.92	7.81	7.81	7.81	7.81

Table 10

Propagation velocity versus distance for decane-air mixture at E_{cu}

ϕ	Initiator pressure (atm)	No. of runs	R(cm)	50	125	175	225	300	375	450	525	575	625
0.92	7.81	6	V(cm/s)	2002	1878	1780	1726	1608	1582	1526	1504	1464	1388
			σ(cm/s)	17.3	30.7	15.6	16.2	12.6	7.8	24.2	34.7	36.9	71.0
1.18	2.36	10	V(cm/s)	1420	1676	1601	1580	1535	1579	1543	1539	1539	1516
			σ(cm/s)	58.6	72.3	21.9	27.3	6.9	17.5	22.7	15.8	20.5	12.8
1.70	2.70	8	V(cm/s)	1523	1526	1521	1539	1505	1565	1555	1554	1570	1543
			σ(cm/s)	14.1	25.6	30.4	19.0	21.5	21.9	14.1	12.7	27.0	35.6
2.49	3.38	5	V(cm/s)	1627	1585	1585	1573	1525	1580	1571	1581	1569	1542
			σ(cm/s)	58.9	42.4	28.4	35.9	31.6	21.8	4.5	9.6	15.2	5.2
3.27	4.06	6	V(cm/s)	1706	1631	1602	1587	1529	1577	1556	1575	1569	1555
			σ(cm/s)	35.9	32.5	31.7	29.3	23.6	9.6	3.3	15.5	6.7	18.5

V is the average of the propagation velocity under the same experimental conditions.

σ is the standard deviation of the propagation velocity.

Table 11

Propagation velocity versus distance for decane-O_2 mixture at E_{cu}

ϕ	Initiator pressure (atm)	No. of runs	Distance R(cm)	50	125	175	225	300	375	450	525	575	625
0.24	5.76	6	V(cm/s)	1828	1719	1680	1663	1598	1604	1583	1562	1538	1496
			σ(cm/s)	22	38	38	27	43	30	28	21	37	35
0.27	2.02	5	V(cm/s)	1614	1673	1668	1655	1623	1609	1588	1551	1529	1492
			σ(cm/s)	41	41	50	59	66	51	58	50	46	62
0.38	2.02	4	V(cm/s)	1639	1799	1804	1803	1781	1745	1704	1661	1648	1626
			σ(cm/s)	140	12	13	6	6	8	9	11	20	24
0.56	2.02	4	V(cm/s)	1829	1951	1956	1956	1932	1880	1829	1803	1765	1748
			σ(cm/s)	10	13	13	4	2	6	8	8	6	9
0.74	2.02	6	V(cm/s)	1876	1989	2016	2019	1991	1941	1881	1841	1832	1801
			σ(cm/s)	8	8	1	4	2	4	2	3	10	6

Table 12

Some detonation and initiation properties of decane-air mixtures

Equivalence ratio ϕ	0.92	1.18	1.70	2.49	3.27
Theoretical D_{CJ} (m/s) (all gaseous)	1770	1829	1795	1648	1487
Experimental D_{CJ} (m/s) at E_{cu}	1388	1516	1543	1542	1555
Critical initiator pressure (atm)	7.81	2.36	2.70	3.38	4.06
Blast wave energy (MJ/m^2)	33.10	9.23	10.65	13.54	16.47
Velocity deficit (percentage)	21.6	17.11	14.04	6.4	-4.6
Shock decay velocity (at the end of tube) (m/s)	1122	642	682	723	824
Calculated ratio of specific heats γ behind detonation	1.177	1.183	1.251	1.293	1.303
Initial density of the mixture ρ_o (gm/cm^3)	1.236×10^{-3}	1.252×10^{-3}	1.284×10^{-3}	1.330×10^{-3}	1.376×10^{-3}
Heat of combustion (cal/gm)	596.8	686.7	503.0	422.4	413.6
Blast wave radius R* (cm)	536	128	171	288	346

Table 13

Some detonation and initiation properties of decane-oxygen mixtures

Equivalence ratio ϕ	0.24	0.27	0.38	0.56	0.74
Theoretical D_{CJ} (m/s) (all gaseous)	1754	1798	1934	2082	2200
Experimental D_{CJ} (m/s) at E_{cu}	1496	1492	1626	1748	1801
Critical initiator pressure (atm)	5.76	2.02	2.02	2.02	2.02
Blast wave energy (MJ/m^2)	23.92	7.81	7.81	7.81	7.81
velocity deficit (percentage)	14.79	17.02	15.93	16.04	18.14
Shock decay velocity (at the end of tube) (m/s)	947	600	600	600	t00
Ratio of specific heat γ	1.168	1.164	1.170	1.191	1.208
Initial density of the mixture ρ_o (gm/cm^3)	1.376×10^{-3}	1.388×10^{-3}	1.417×10^{-3}	1.465×10^{-3}	1.514×10^{-3}
Heat of combustion (cal/gm)	733.45	748.70	800.61	871.53	843.02
Blast wave radius R* (cm)	283.22	89.87	82.32	73.14	73.17

Table 14

Propagation velocity versus distance for decane-air mixtures

ϕ	Initiator pressure (atm)	No. of runs	R(cm)	25	50	75	125	175	225	300	375	450	525	575	625
1.18	4.40	7	V(cm/s)	1805		1775	1703	1679	1652	1622	1618	1569	1563	1548	
			σ(cm/s)	27		28	14	9	16	7	11	24	26	32	
1.70	4.40	6	V(cm/s)	1795		1747	1691	1686	1628	1626	1640	1579	1574	1582	
			σ(cm/s)	9		25	11	60	39	6	63	24	12	13	
2.49	4.40	6	V(cm/s)	1777		1683	1616	1574	1550	1534	1576	1547	1575	1581	
			σ(cm/s)	12		11	41	18	7	17	17	6	14	20	
3.27	4.40	5	V(cm/s)	1762		1607	1503	1485	1472	1485	1536	1530	1545	1615	
			σ(cm/s)	14		12	14	19	24	4	4	4	14	45	

Table 15

Propagation velocity versus distance for decane-O_2 mixtures

ϕ	Initiator pressure (atm)	No. of runs	Distance R(cm)	25	50	75	125	175	225	300	375	450	525	575	625
0.27	4.40	7	V(cm/s)	1842		1827	1779	1722	1694	1658	1601	1557	1515	1500	
			σ(cm/s)	18		28	12	14	17	31	41	21	18	31	
0.38	4.40	10	V(cm/s)	1914		1917	1890	1839	1778	1782	1727	1662	1611	1576	
			σ(cm/s)	19		33	51	61	83	59	58	57	54	59	
0.56	4.40	5	V(cm/s)	1972		1997	1969	1932	1894	1867	1811	1745	1693	1697	
			σ(cm/s)	15		13	12	14	14	19	29	14	15	40	
0.74	4.40	9	V(cm/s)	2007		2073	2048	2012	1975	1934	1864	1802	1760	1742	
			σ(cm/s)	36		26	19	12	16	15	20	17	18	23	

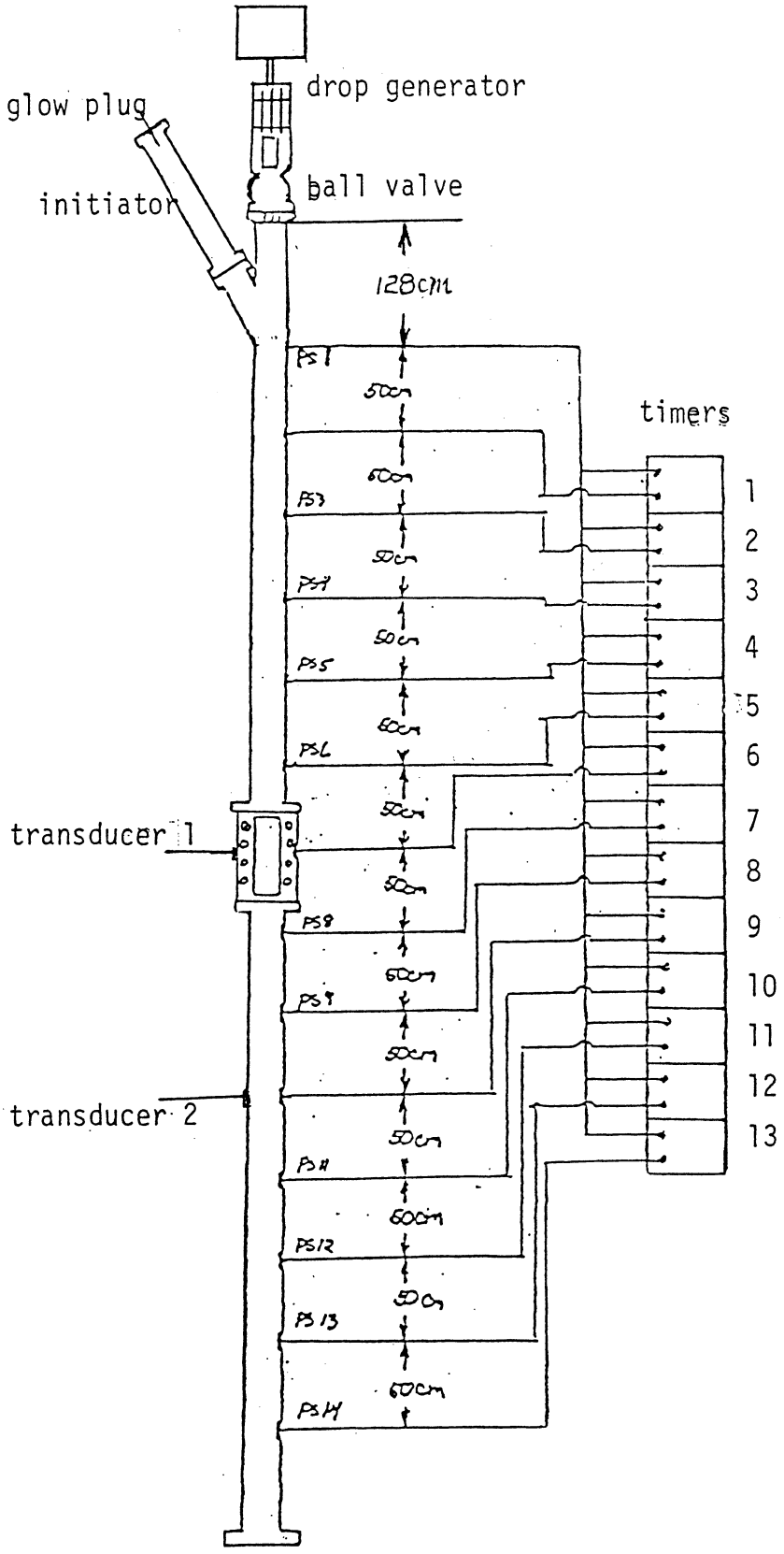

Figure 1. Schematic of the Shock Tube

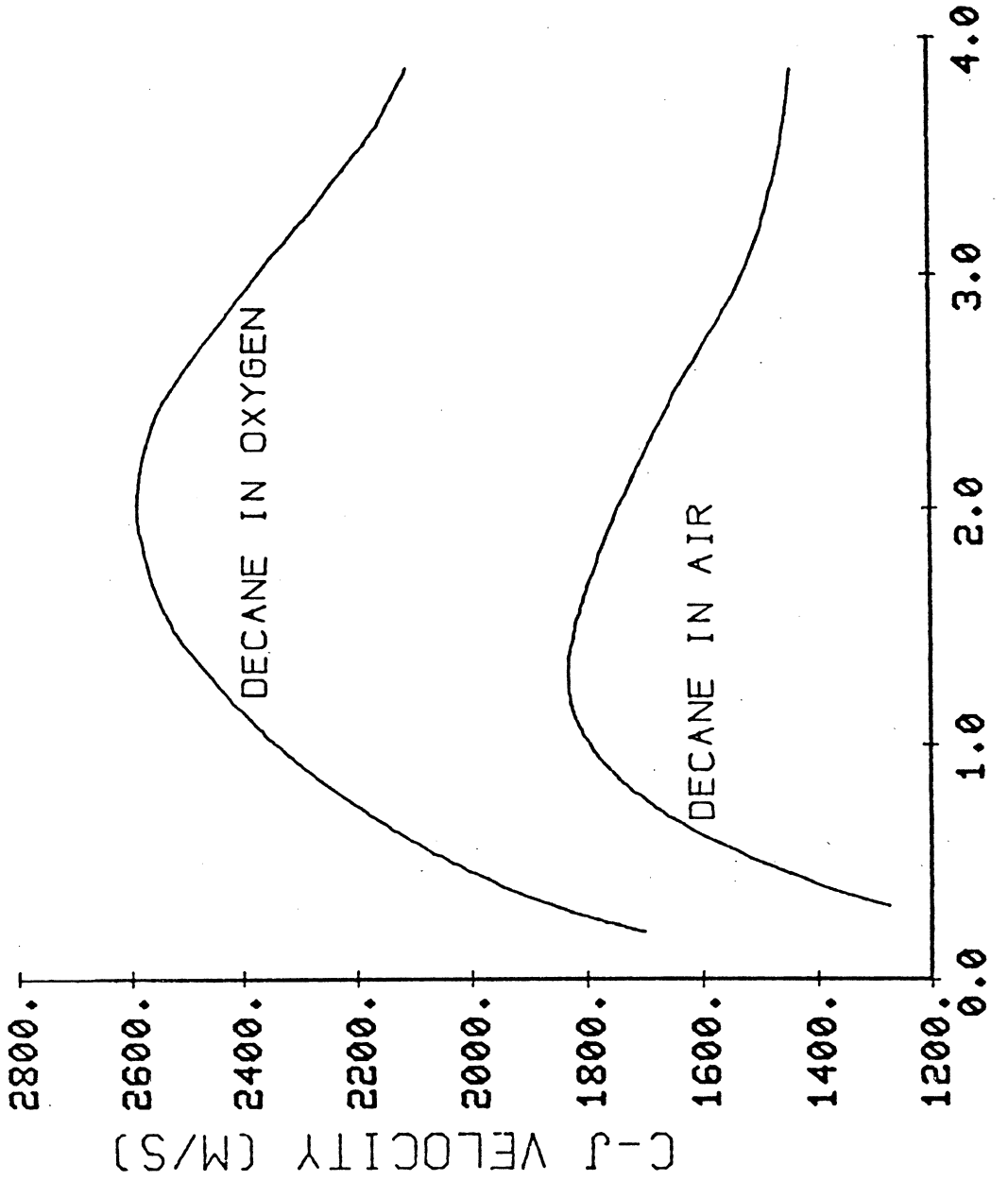

Figure 2. Chapman-Jouguet velocity as the function of ϕ (according to Gordon McBride).

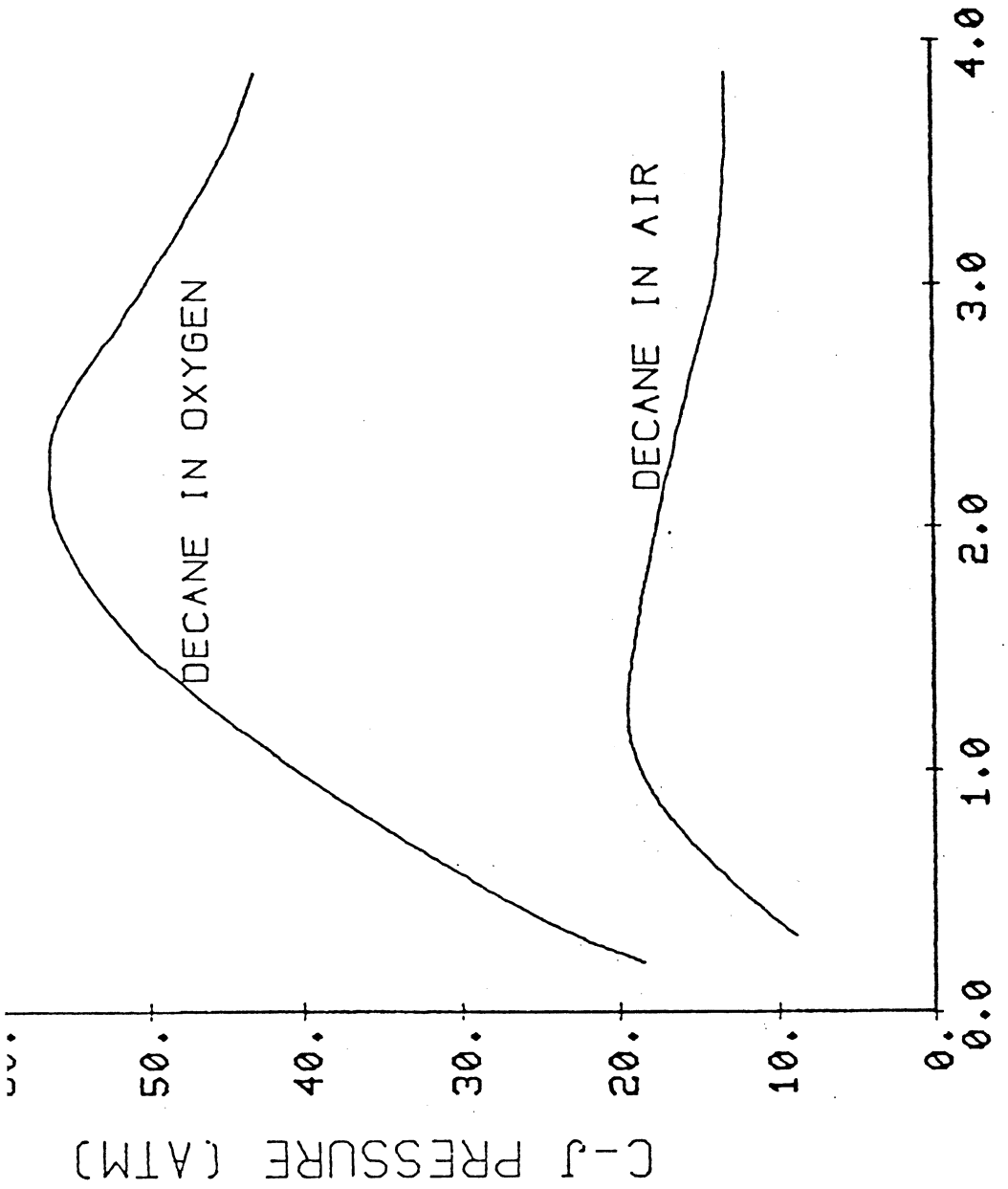

Figure 3. C-J Pressure as the Function of ϕ (according to Gordon McBride)

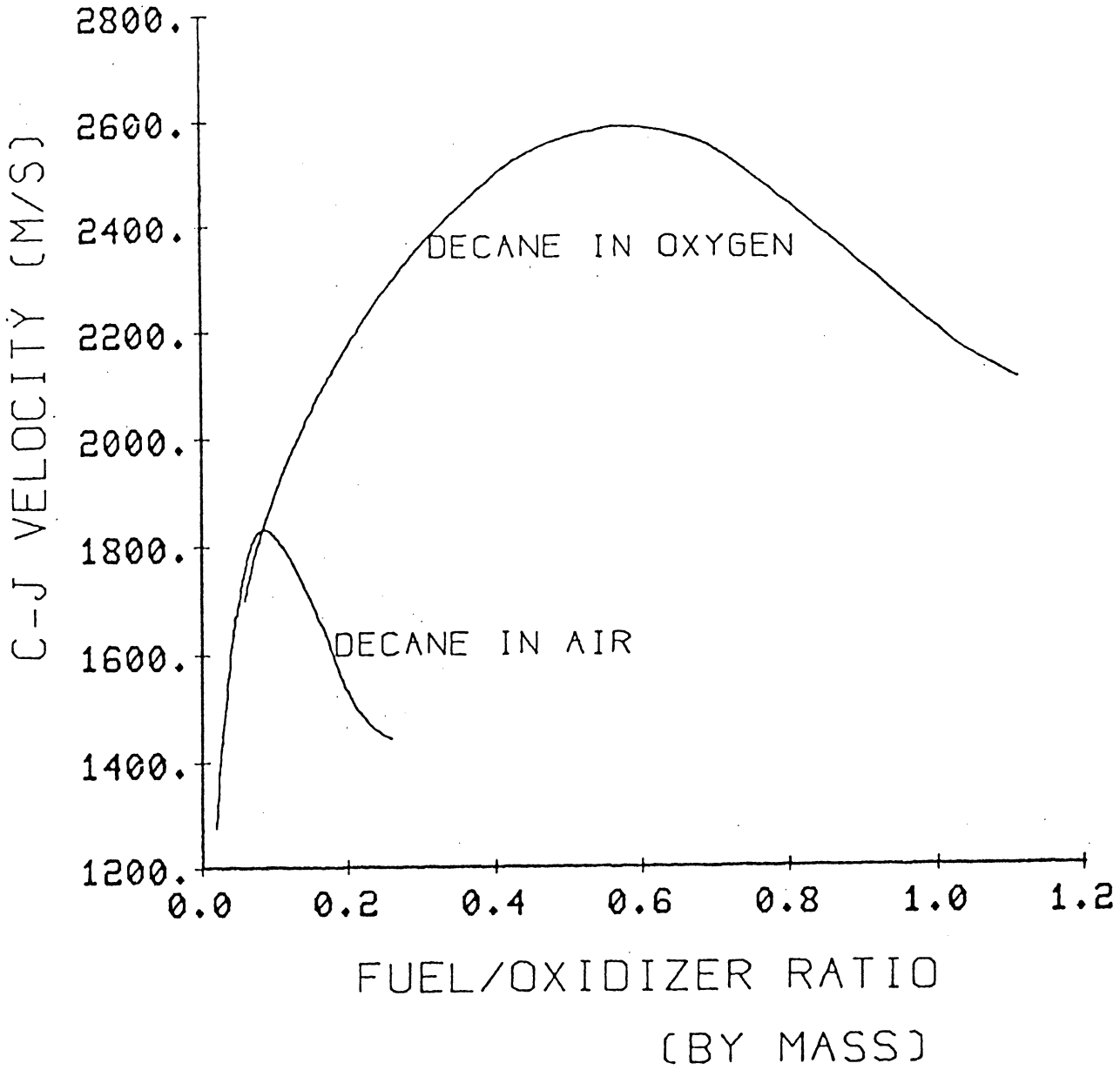

Figure 4. Chapman-Jouguet Velocity Versus

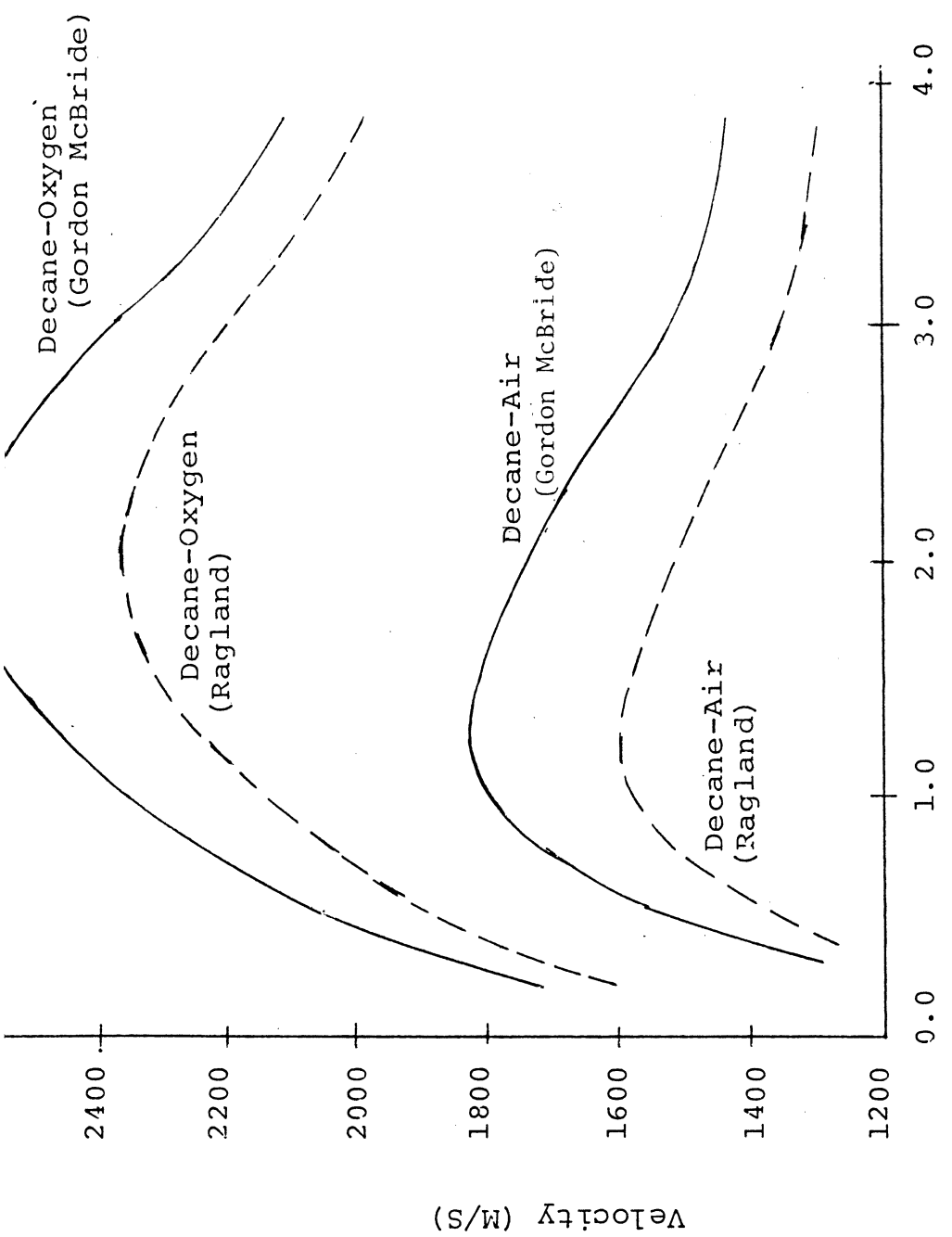

Figure 5. Detonation velocity obtained by Gordon McBride and Ragland, et al.

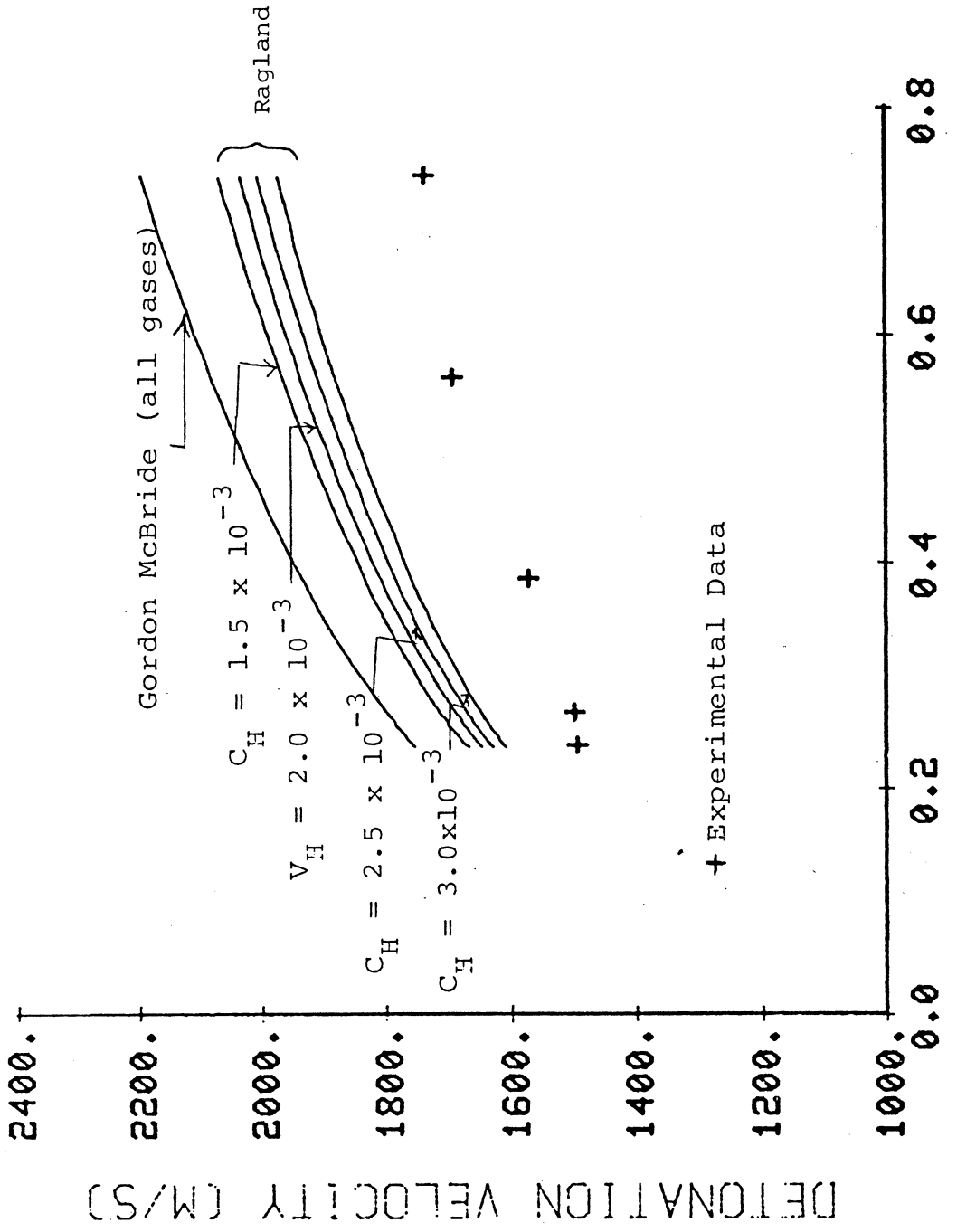

Figure 6. Effect of C_H on D_{CJ} (decane-O_2, t_3 = 50μs)

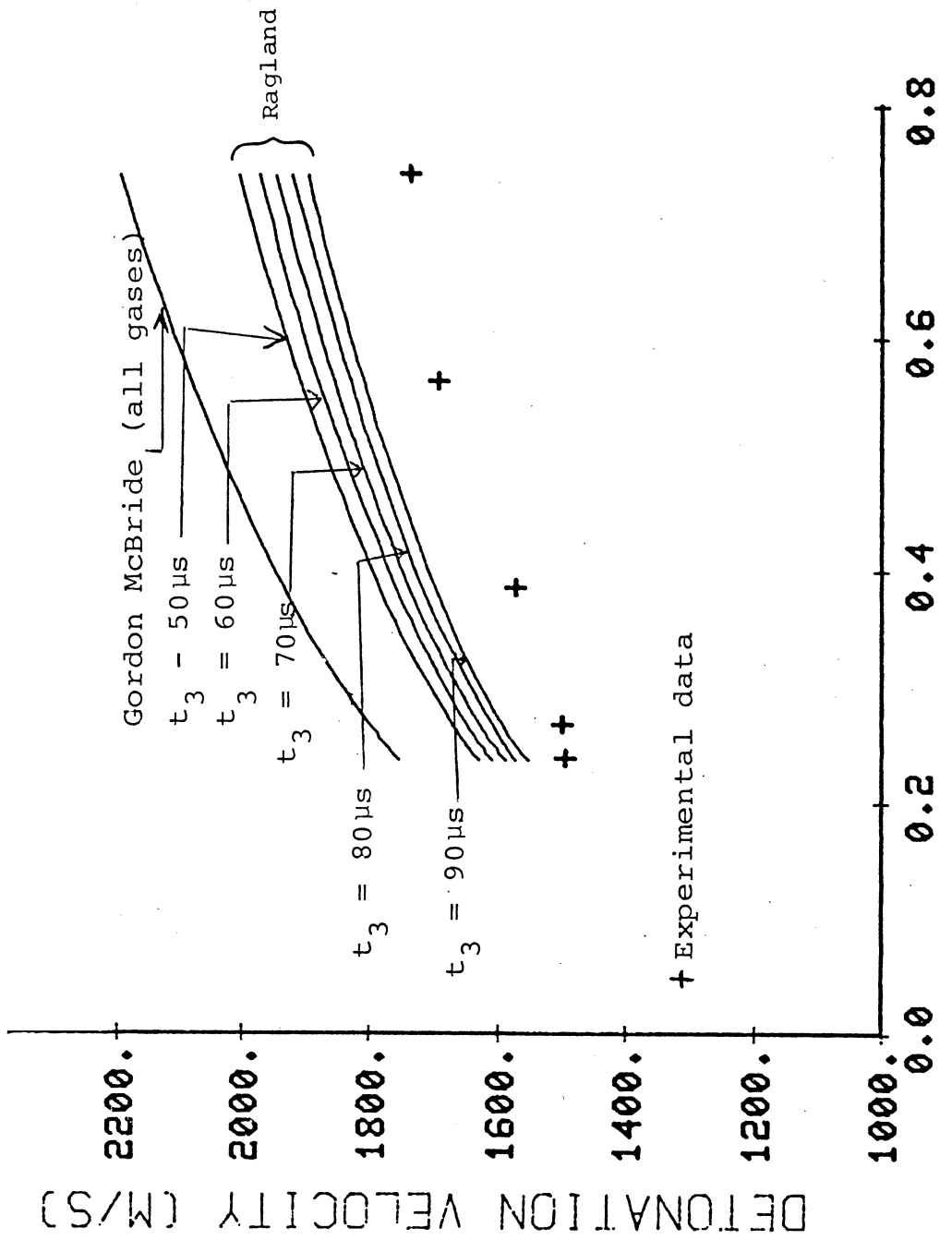

Figure 7. Effect of t_3 on D_{CJ} (decane - O_2, $C_H = 2.5 \times 10^{-3}$)

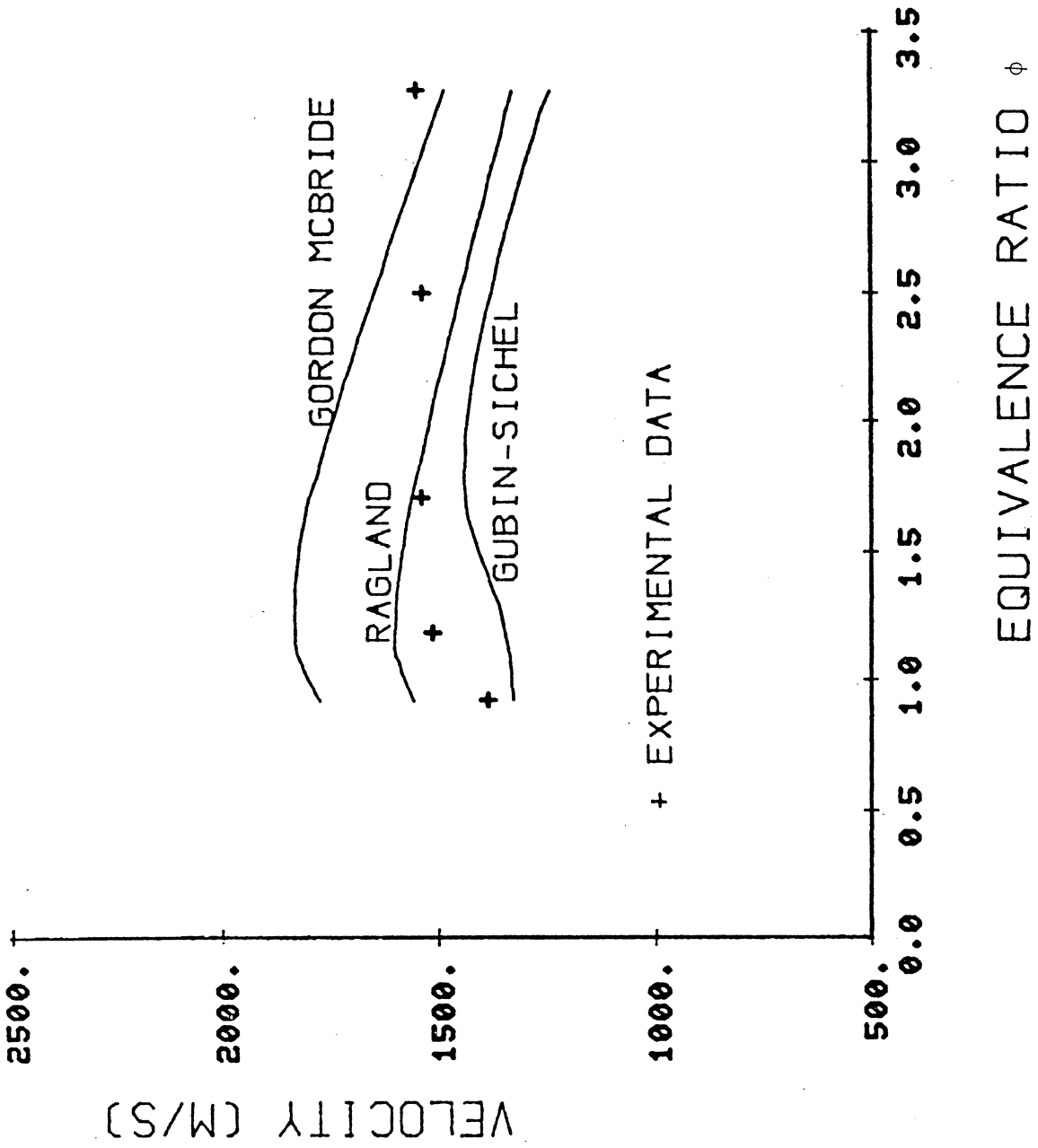

Figure 8. Detonation velocity versus ϕ for decane-air mixture (according to different methods)

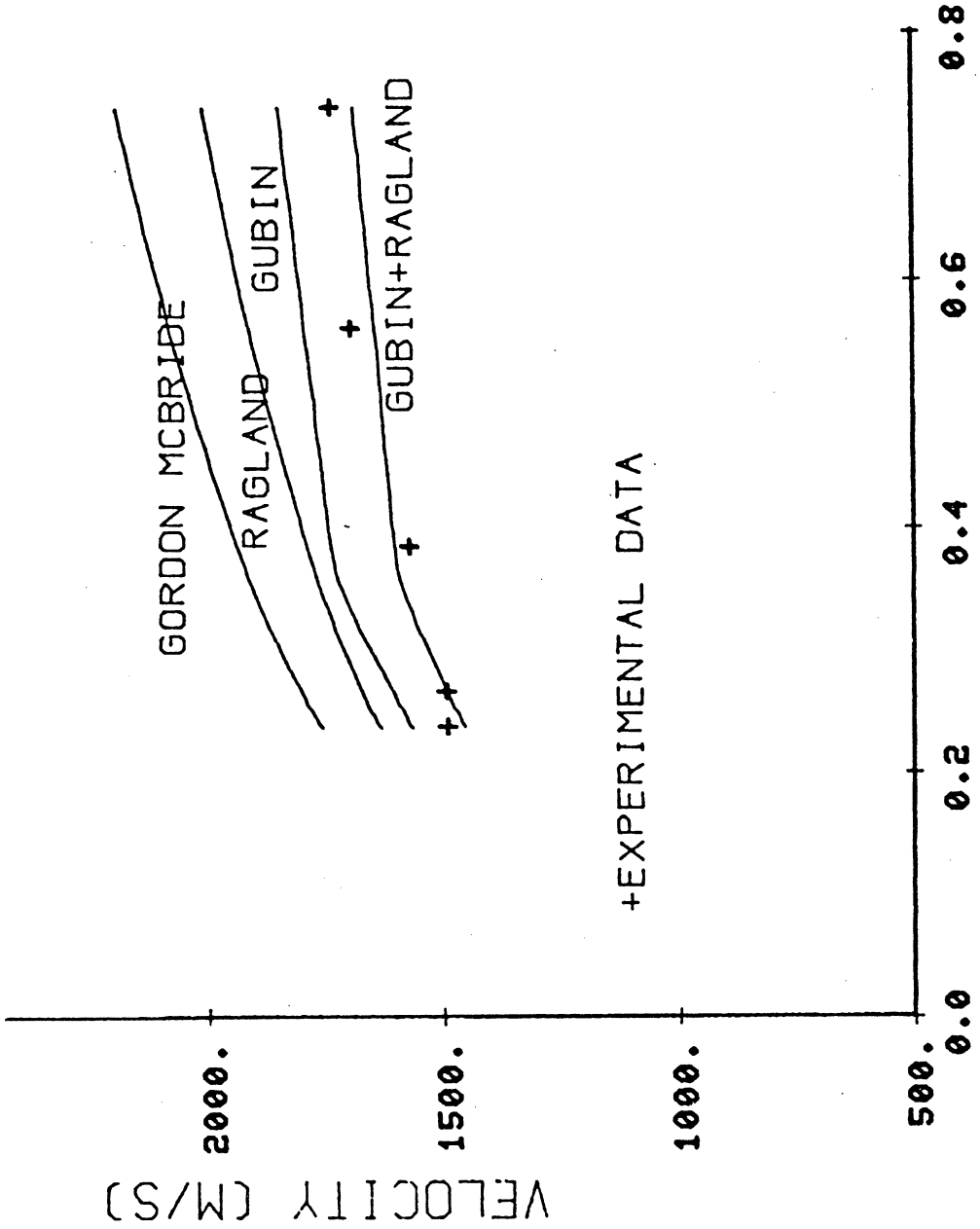

Figure 9. Detonation velocity versus ϕ for decane-O_2 mixture (according to different methods)

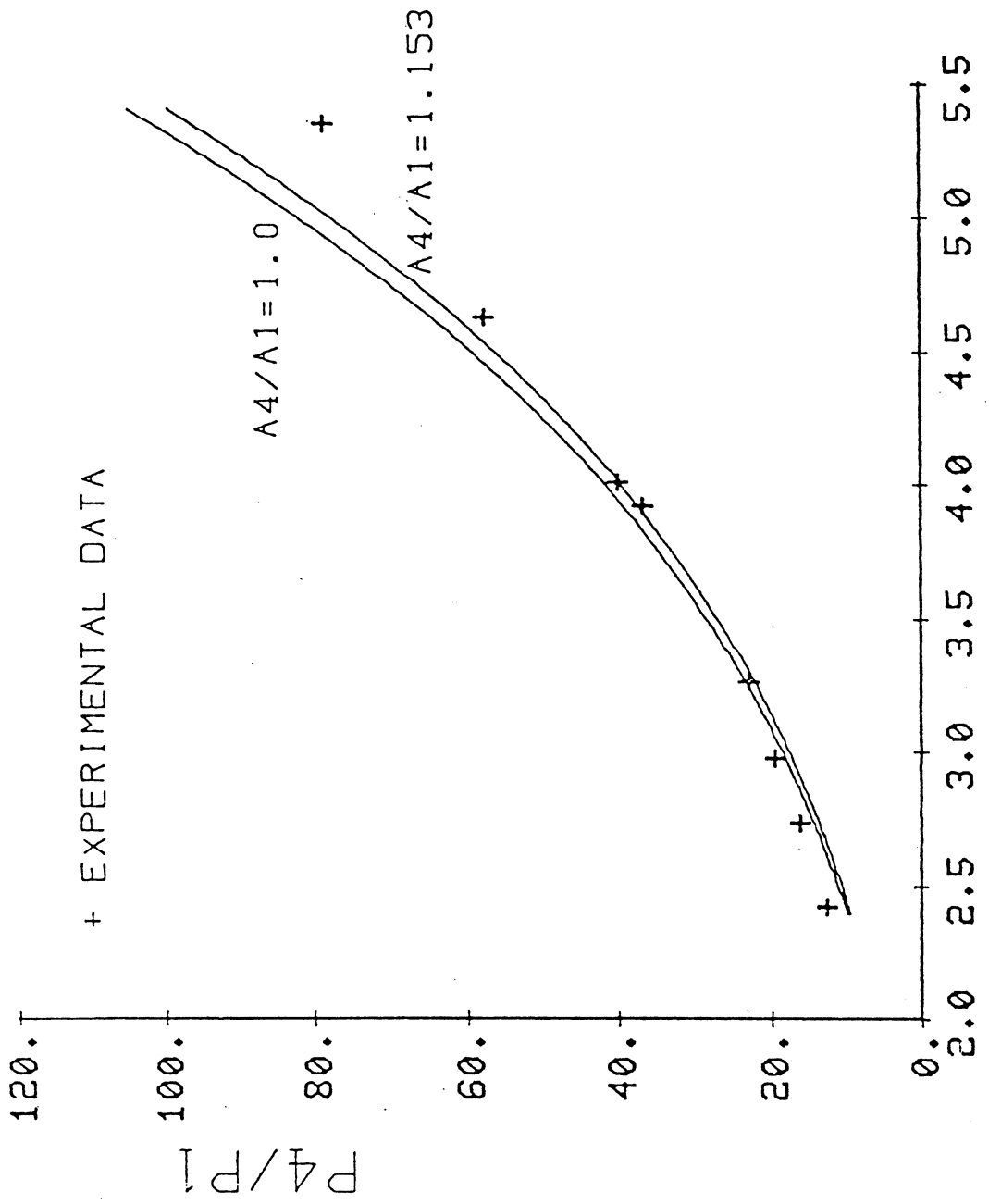

Figure 10. Pressure Ratio Versus Initiation Mach Number

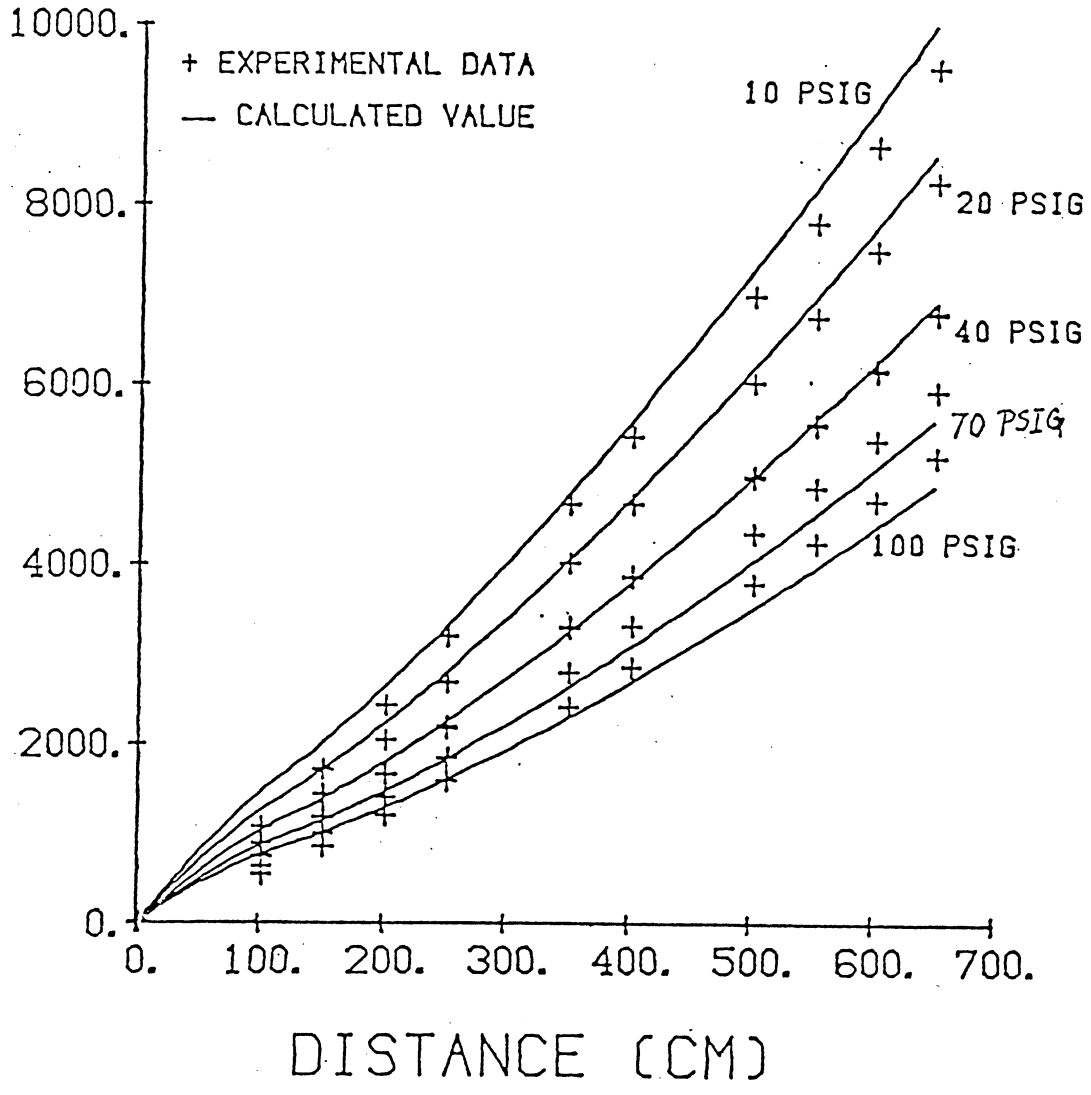

Figure 11. The Trajectories of the Shock Front Propagating in Non-Reactive Mixtures

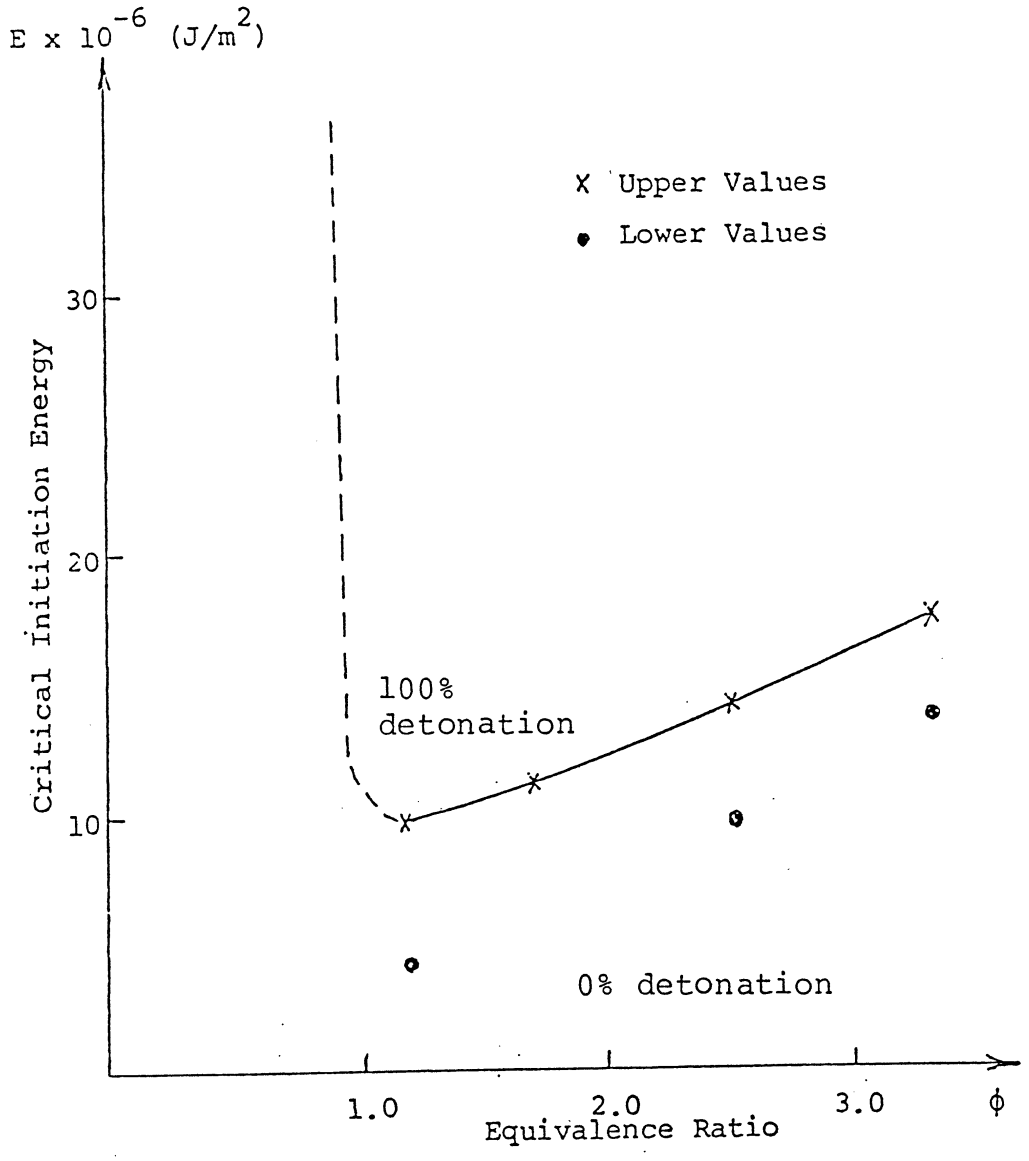
E x 10^-6 (J/m^2)
Critical Initiation Energy
30
20
10
X Upper Values
• Lower Values
100% detonation
0% detonation
1.0
2.0
3.0
ϕ
Equivalence Ratio

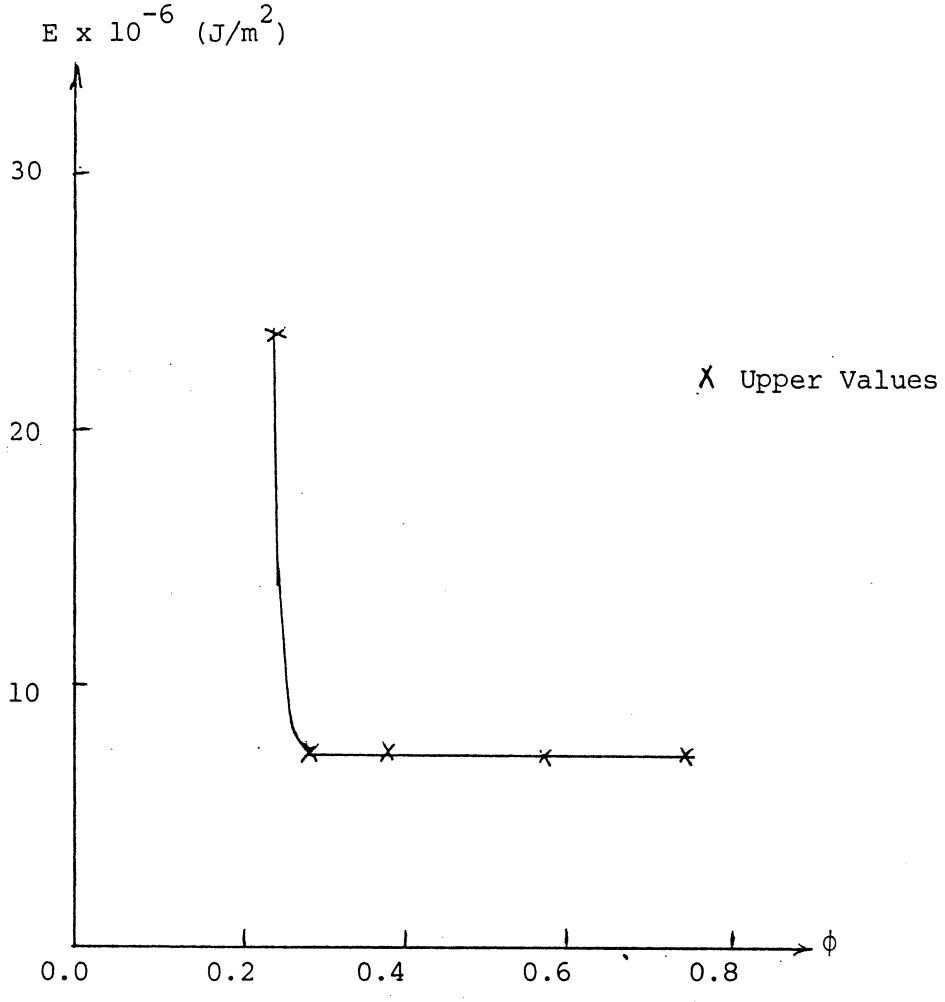

Figure 13. Critical initiation energy of decane-oxygen mixture

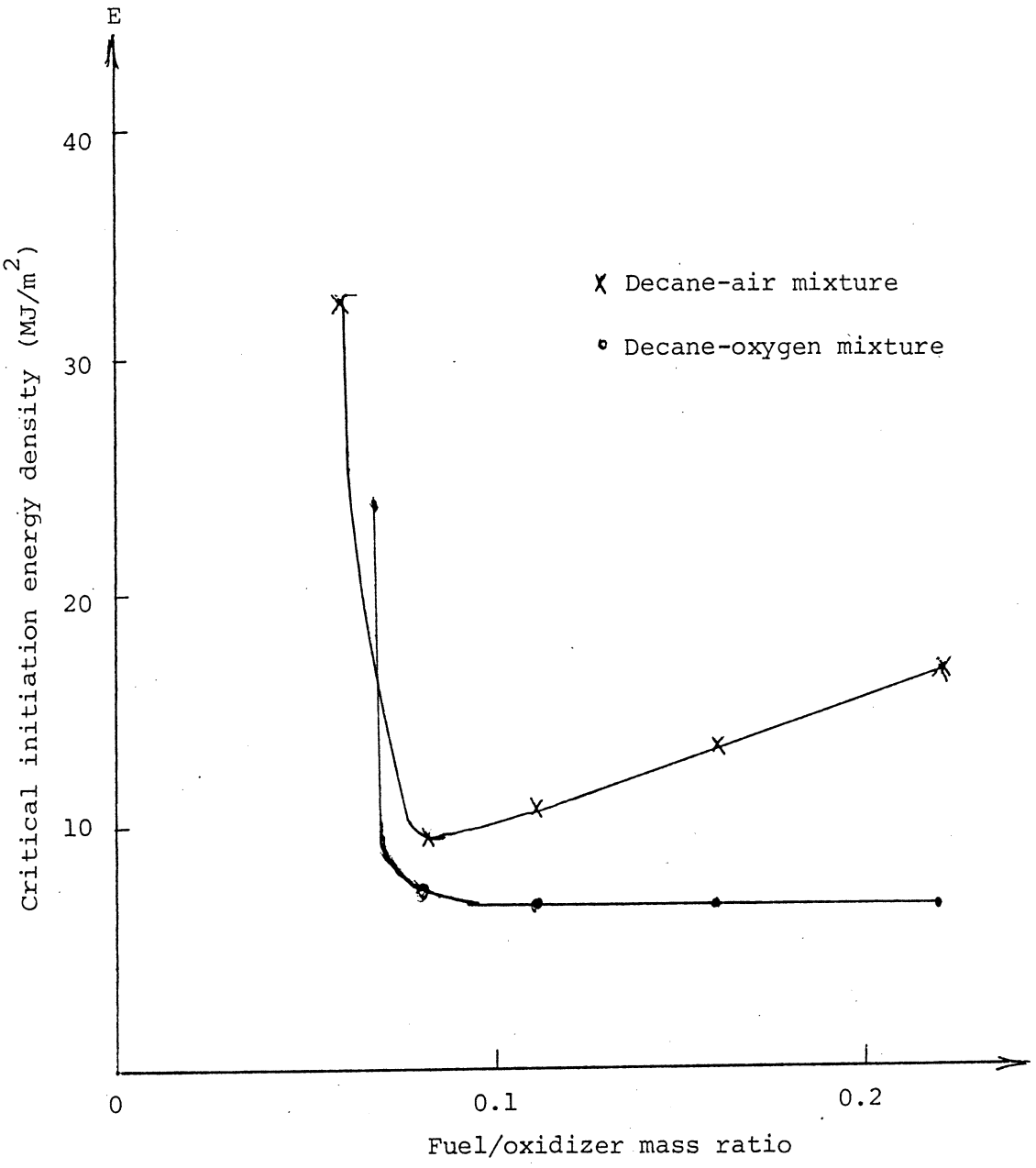

Figure 14. Critical initiation E_{cu} energy against fuel/oxidizer ratio

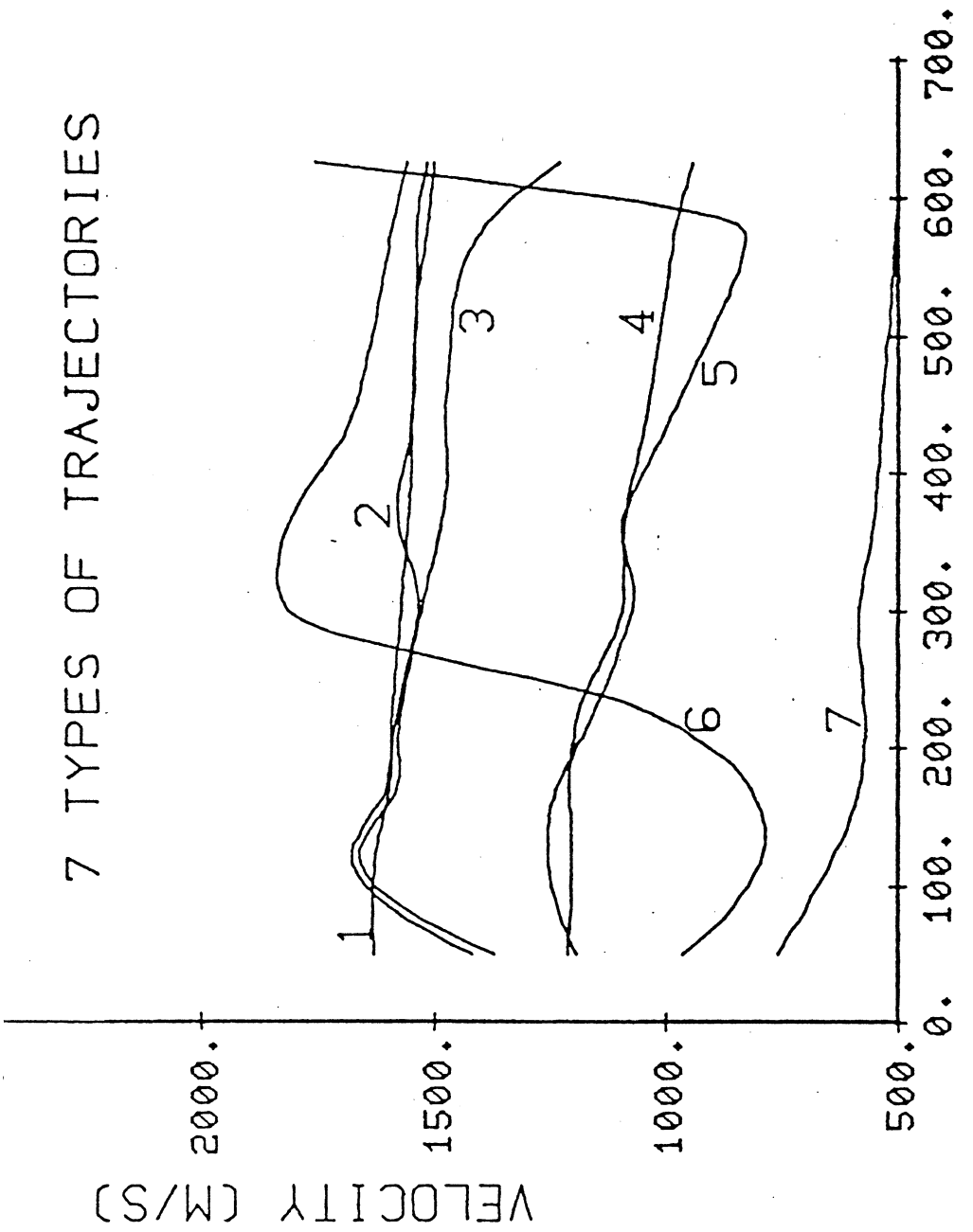

Figure 15. 7 types of velocity trajectories.

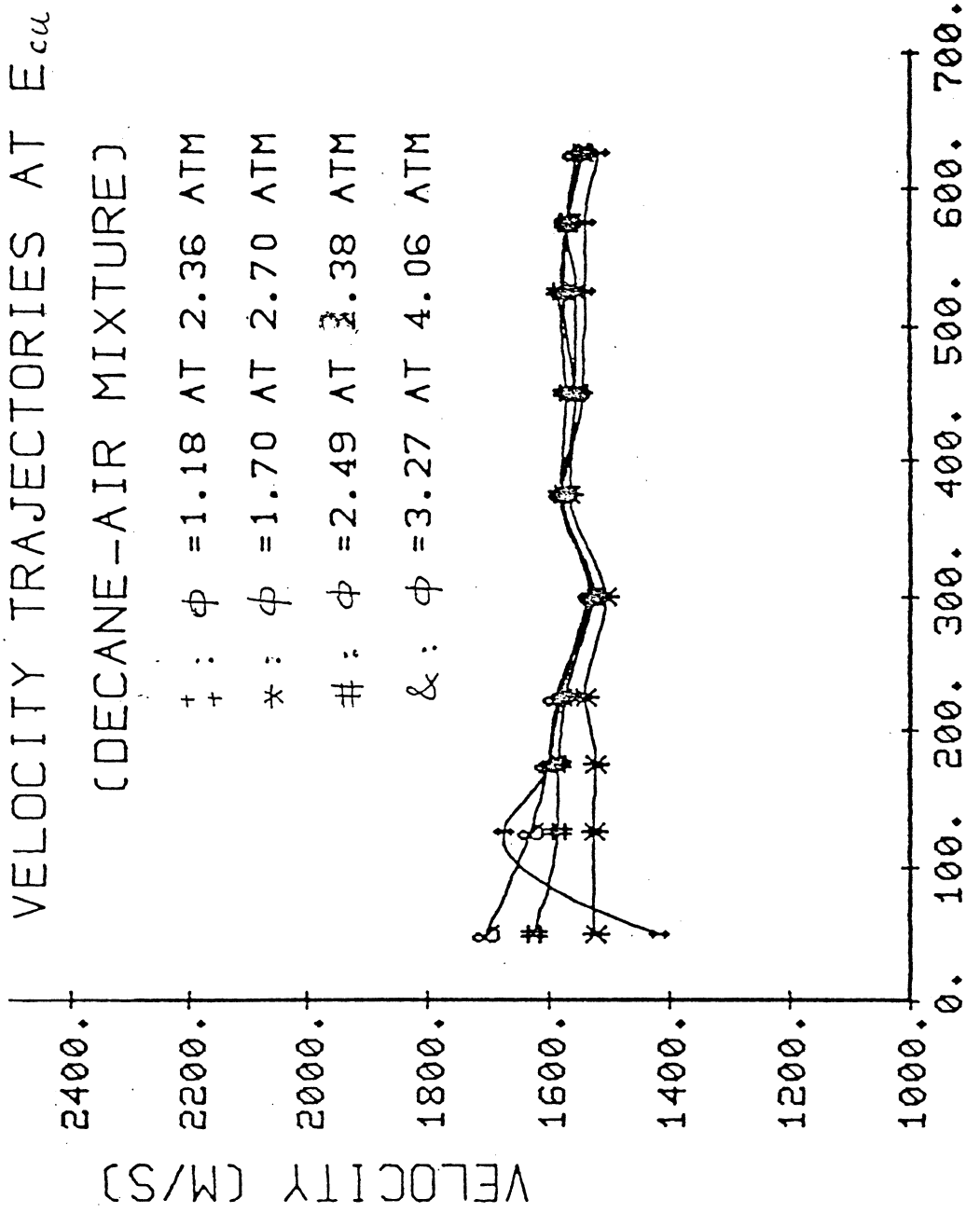

Figure 16. Velocity trajectories at E_{cu} (for decane-air mixture)

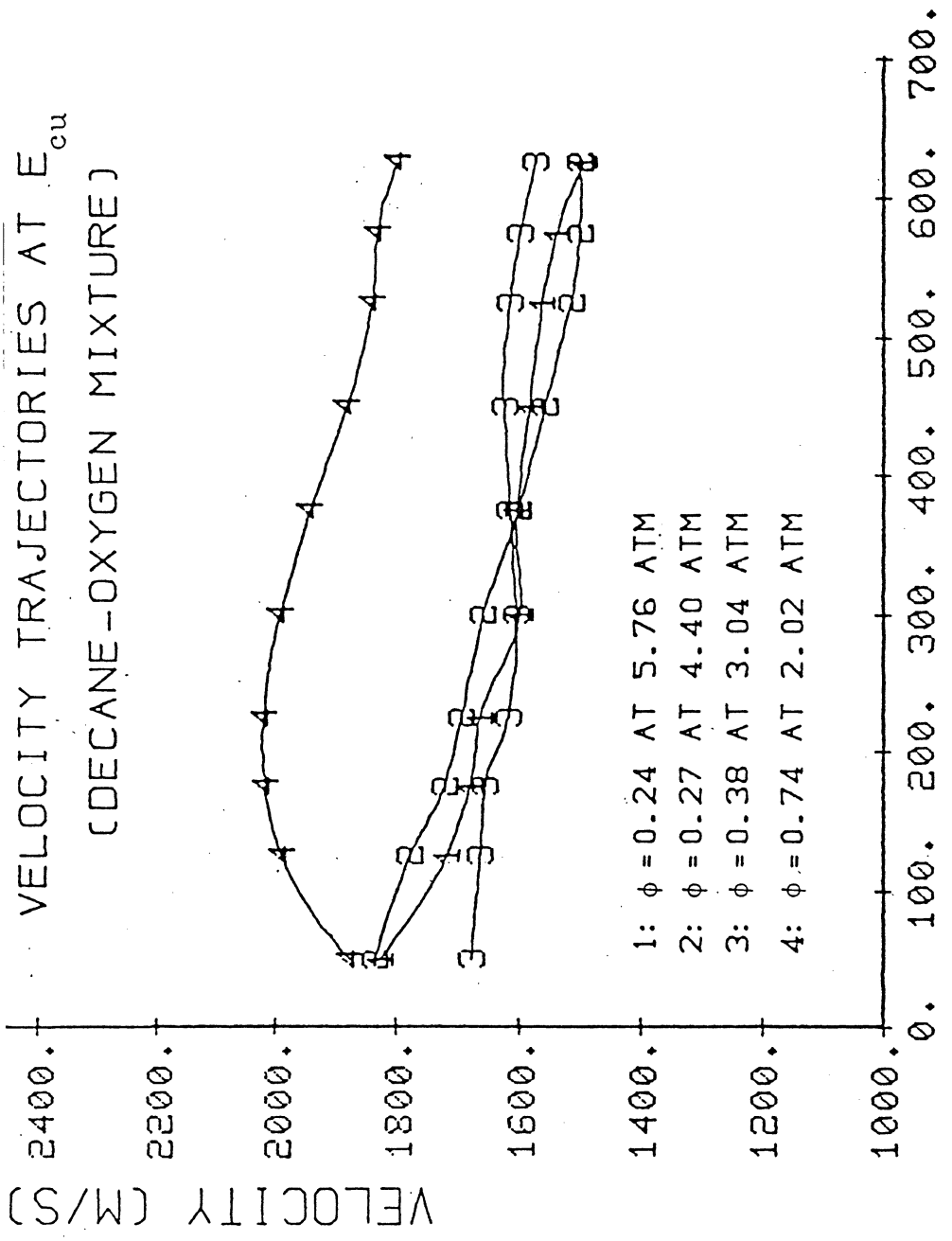

Figure 17. Velocity trajectories at E_{cu} (for decane-oxygen mixture).

(a) ϕ = 0.92
initiator pressure
7.81 atm
upper trace
R = 300 cm
20.2 atm/div.;
100 μsec/div.
lower trace
R = 450 cm
20.2 atm/div;
100 μsec/div.

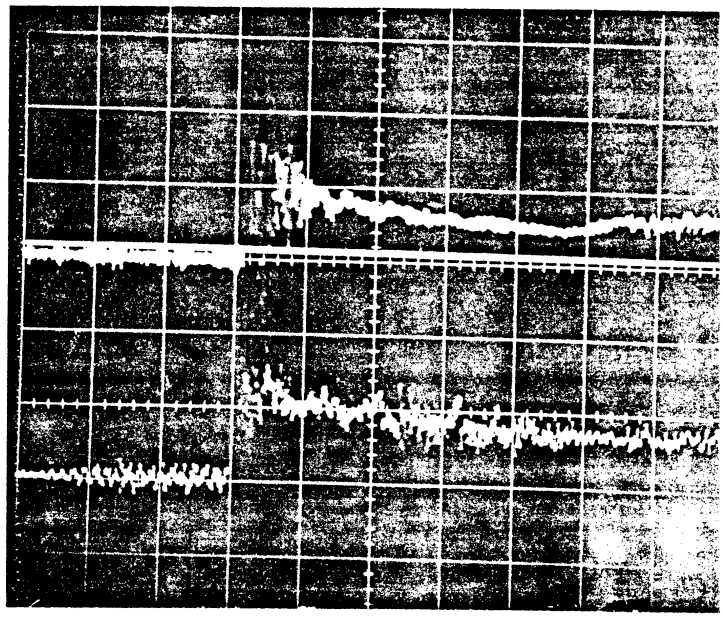

(b) ϕ = 1.18
initiator pressure
2.36 atm
upper trace
R = 300 cm
20.2 atm/div.;
100 μsec/div.
lower trace
R = 450 cm
20.2 atm/div.;
100 μsec/div.

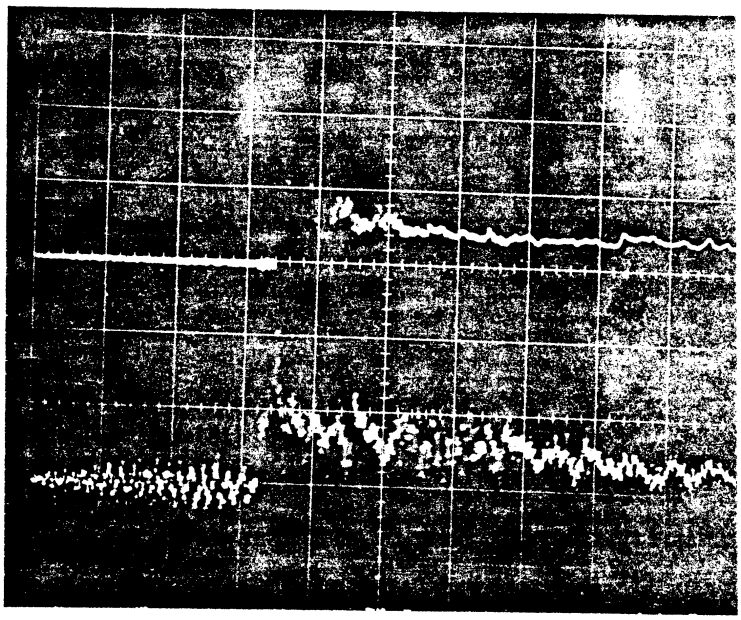

(c) ϕ = 1.70
initiator pressure
2.70 atm
upper trace
R = 300 cm
20.2 atm/div.;
100 μsec/div.
lower trace
R = 450 cm
20.2 atm/div.;
100 μsec/div.

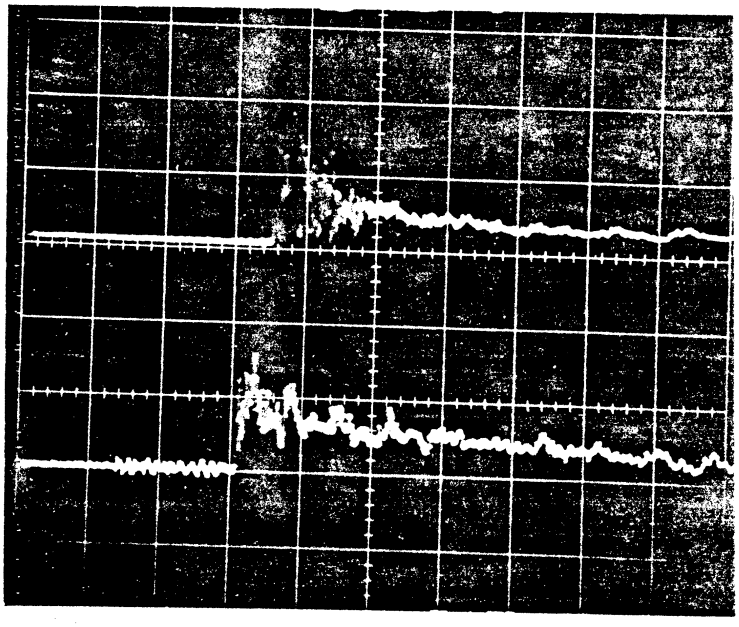

Figure 18. Pressure traces of detonation in decane-air mixtures.

(d) ϕ = 2.49

initiator pressure
3.38 atm
upper trace
R = 300 cm
20.2 atm/div.;
100 μs/div.
lower trace
R = 450 cm
20.2 atm/div.;
100 μs/div.

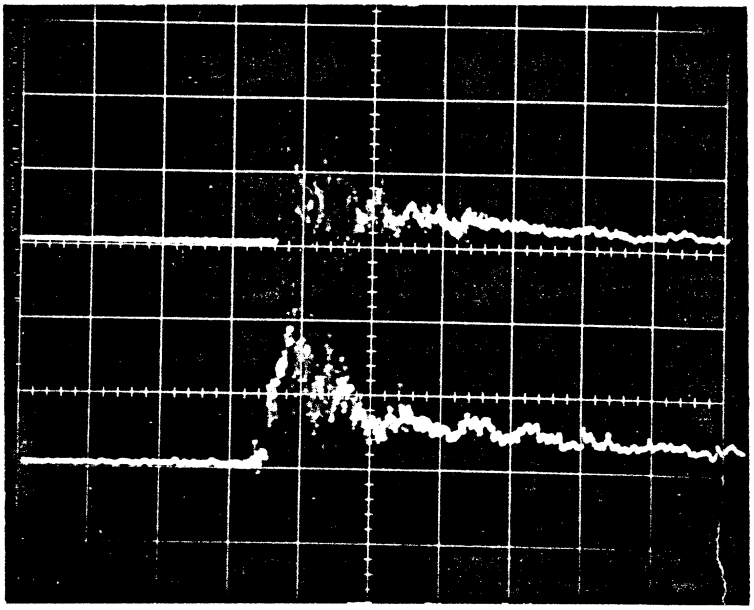

(e) ϕ = 3.27

initiator pressure
4.06 atm
upper trace
R = 300 cm
20.2 atm/div.;
100 μs/div.
lower trace
R = 450 cm
20.2 atm/div.;
100μs/div.

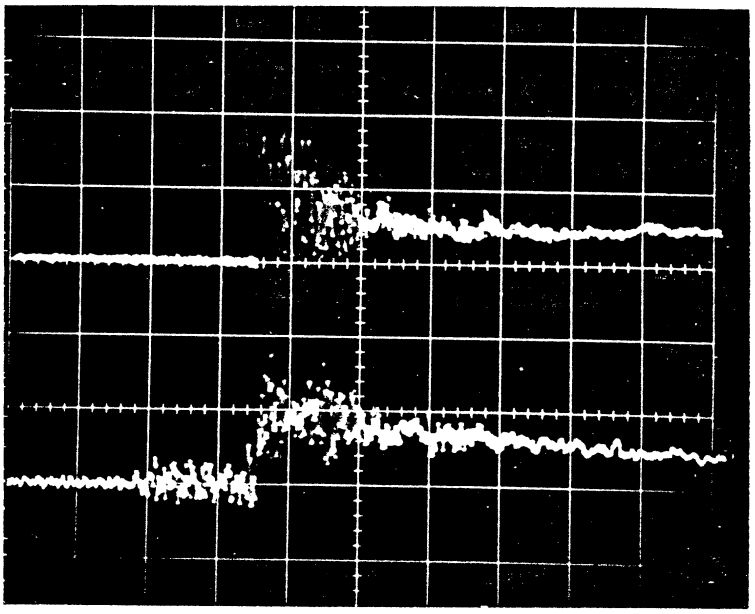

Figure 18 (continued). Pressure traces of detonation in decane-air mixtures.

(a) ϕ = 0.24
initiator pressure
5.76 atm
upper trace
R = 300 cm
20.2 atm/div.;
100 μsec/div.
lower trace
R = 450 cm
20.2 atm/div.;
100 μsec/div

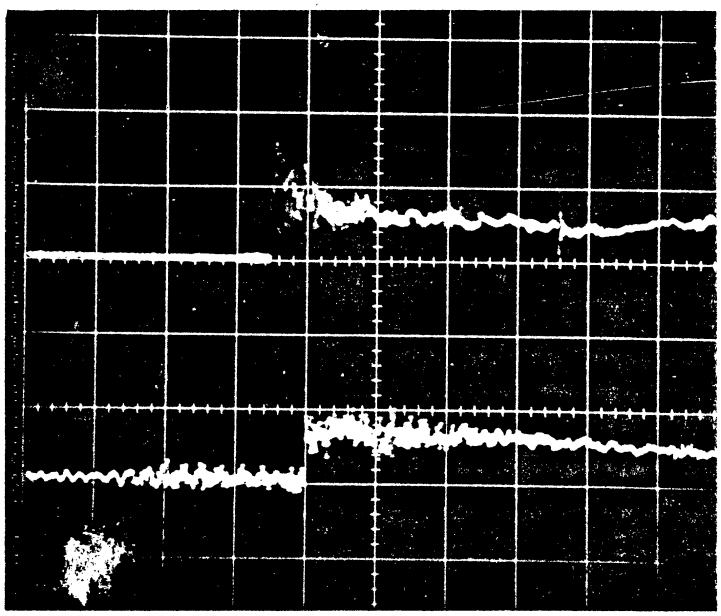

(b) ϕ = 0.38
initiator pressure
3.04 atm
upper trace
R = 300 cm
20.2 atm/div.;
100μsec/div.
lower trace
R = 450 cm
20.2 atm/div.;
100 μsec/div.

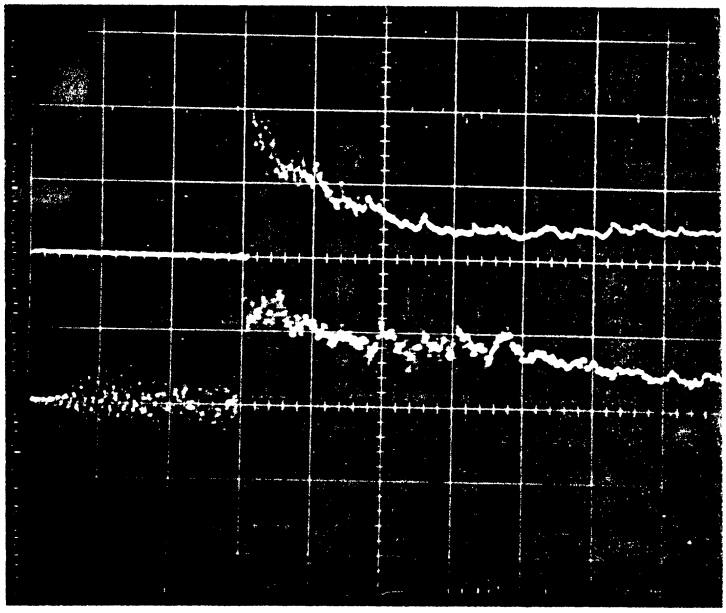

(c) ϕ = 0.74
initiator pressure
2.02 atm
upper trace
R = 300 cm
20.2 atm/div.;
100 μsec/div.
lower trace
R = 450 cm
20.2 atm/div.;
100 μsec/div.

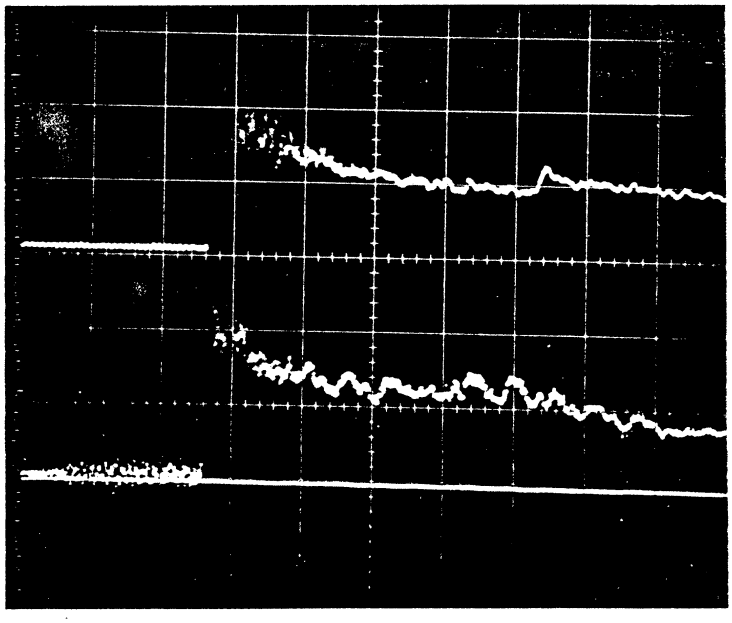

Figure 19. Pressure traces of detonation in decane-O_2 mixtures.

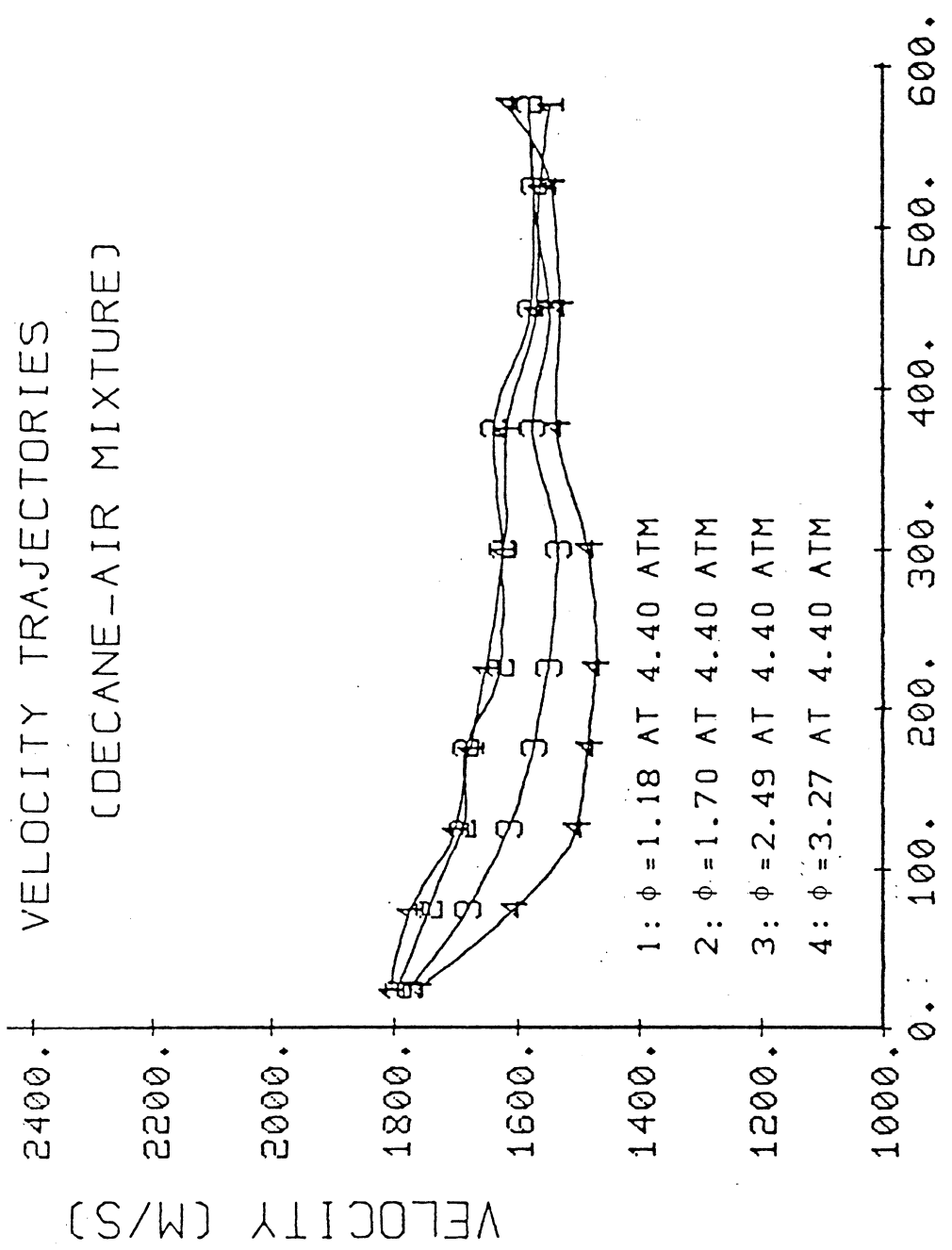

Figure 20. Velocity trajectories at 440 atm (decane-air mixture).

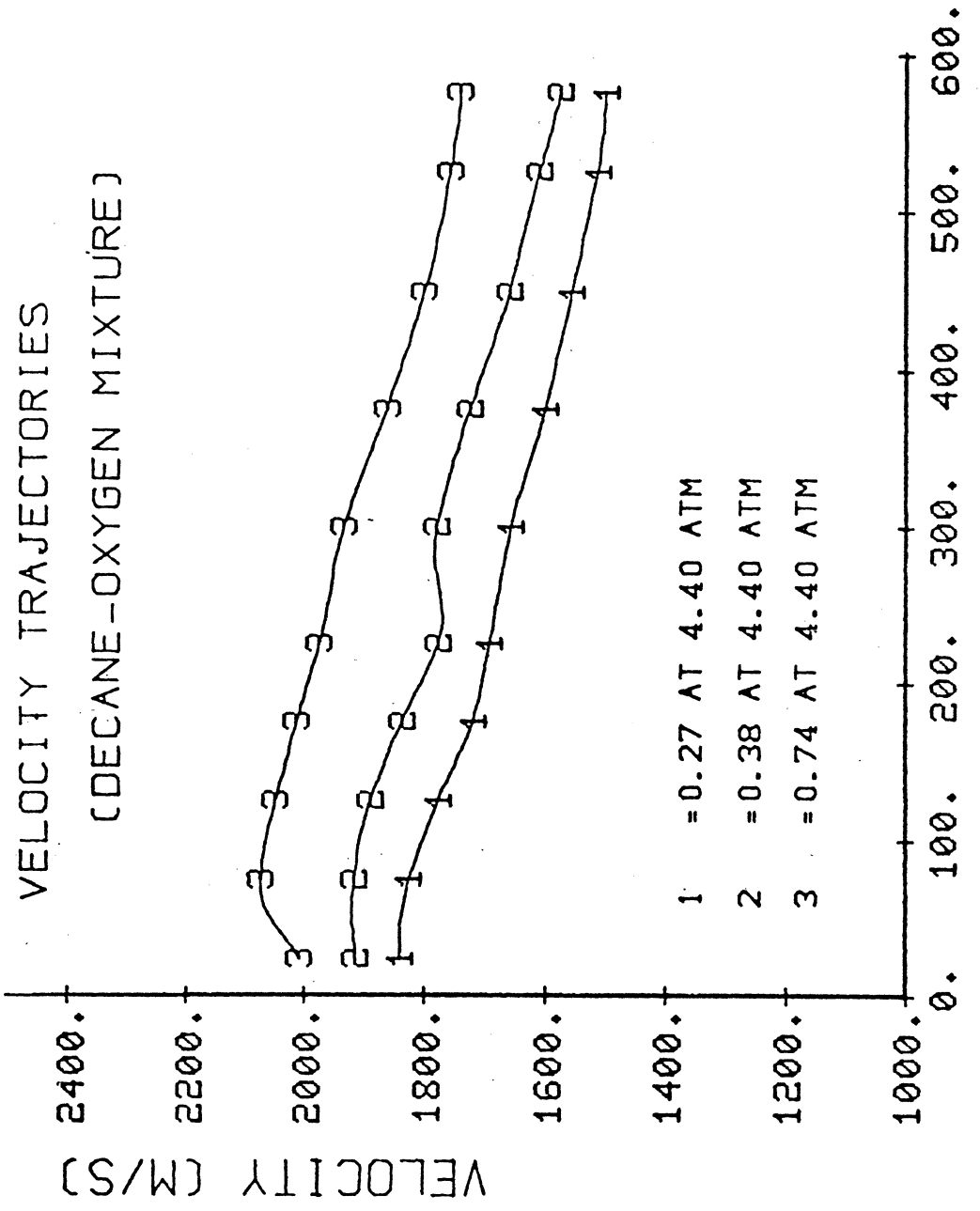

Figure 21. Velocity trajectories at 440 atm (decane-O_2 mixture).